Science and Technology Indonesia
e-ISSN:2580-4391 *p*-ISSN:2580-4405
Vol. 11, No. 3, July 2026

Research Paper

Preparation of Carrageenan/Chitosan/Curcumin Hydrogel Films: Physicochemical Characterization and In Vitro Evaluation as a Promising Diabetic Wound Dressing

Sry Agustina[1,2*], Saidun Fiddaroini[1], Ahmad Luthfi Fahmi[1], Ruslan[2], Elvina Dhiaul Iftitah[1], Moh. Farid Rahman[1], Akhmad Sabarudin[1,3*]

[1]*Department of Chemistry, Faculty of Science, Brawijaya University, Malang, East Java, 65145, Indonesia*
[2]*Department of Chemistry Education, Faculty of Teacher Training and Education, Nggusuwaru University, Bima, West Nusa Tenggara, 84119, Indonesia*
[3]*Research Center for Advanced System and Material Technology, Brawijaya University, Malang, East Java, 65145, Indonesia*
*__Corresponding author__: sryagustina@student.ub.ac.id, sabarjpn@ub.ac.id

Abstract
Wound dressings with their physical characteristics that can maintain moisture and their active content which possesses antibacterial and antioxidant properties, represent a crucial solution in addressing the delayed healing of diabetic wounds. For this purpose, in this work we prepared hydrogel films made from a combination of carrageenan, chitosan, and curcumin, and subsequently evaluated their performance for potential application as the diabetic wound dressings. There were three hydrogel film formulations fabricated using 0.5% chitosan, 0.05% curcumin, and carrageenan at varying concentrations of 1%, 1.5%, and 2%, which were subsequently designated as A1, A2, and A3, respectively. These films were examined for physical parameters, chemical profiles, antibacterial activity against *Staphylococcus aureus* and *Escherichia coli*, and antioxidant activity (DPPH assay). The A2 film formulation demonstrated optimal characteristics, as evidenced by a high swelling capacity of 1439.67 ± 20.36%, an appropriate moisture content of 20.63 ± 0.49%, a film pH of 6.23 ± 0.31%, favorable degradation behavior of 93.27 ± 1.36%, and a film thickness of 0.20 ± 0.001 mm. This formulation also demonstrated superior antibacterial activity against *Staphylococcus aureus* and *Escherichia coli*, accompanied by strong antioxidant activity (IC_{50} = 74.52 ppm). Such results indicate that the carrageenan/chitosan/curcumin hydrogel film, particularly formulation A2, is a promising smart hydrogel dressing candidate for diabetic wound applications.

Keywords
Carrageenan, Chitosan, Curcumin, Diabetic Wounds, Hydrogel Film

Received: 21 February 2026, Accepted: 8 May 2026
https://doi.org/10.26554/sti.2026.11.3.994-1015

1. INTRODUCTION

Diabetes mellitus is a chronic metabolic disease with a global prevalence that continues to rise significantly. In 2024, the number of patients is estimated to reach 537 million people and is projected to increase by 25% by 2030. This disease is characterized by uncontrolled chronic hyperglycemia, which can lead to serious damage to various vital organs such as the heart, blood vessels, kidneys, eyes, and nervous system (Hossain et al., 2024). One of the most threatening and complex complications is diabetic wounds, which affect approximately 25% of patients during their lifetime and represent the leading cause of non-traumatic amputations worldwide (Rizky et al., 2024).

The healing of diabetic wounds faces highly complex multifactorial challenges, including resistant bacterial infections, tissue necrosis, prolonged chronic inflammation, excessive production of reactive oxygen species (ROS), and significant impairment of angiogenesis (Gao et al., 2021; He et al., 2025). The microenvironment of diabetic wounds is characterized by unique pathological conditions such as high blood glucose levels (hyperglycemia), low pH (acidosis), dramatically increased ROS levels, and abnormal matrix metalloproteinase (MMP) activity (Jin et al., 2026). These factors collectively and synergistically hinder normal wound healing through several mechanisms, including impaired fibroblast proliferation and migration, reduced collagen synthesis, vascular endothelial dysfunction, and decreased levels of growth factors such as vascular endothelial growth factor (VEGF). Hence, the risk of chronic infection and complete healing failure increases significantly (Han et al., 2025).

The limitations of currently available wound care solutions further exacerbate the challenges associated with diabetic wound healing. Conventional wound dressings are unable to respond to the dynamic and specific characteristics of the diabetic wound microenvironment. Another limitation, sterile gauze and traditional bandages tend to adhere strongly to newly formed granulation tissue, causing painful secondary trauma

during removal and failing to maintain optimal moisture levels required for epithelial cell migration and new tissue formation (He et al., 2025). Modern commercial wound dressings such as foam dressings, alginate dressings (Sweeney et al., 2012; Boateng et al., 2008), and silver dressings offer good exudate absorption capacity but are generally passive (Nešporová et al., 2020), lacking adequate inherent antimicrobial properties and responsiveness to physiological changes within the wound site.

Further analysis reveals that currently available wound dressing systems are unable to release therapeutic agents in a controlled manner or undergo adaptive material degradation in response to changes within the diabetic wound microenvironment. These limitations can lead to improper pharmacological application, reduced therapeutic efficacy, wastage of wound dressings, and may even trigger antimicrobial resistance (Chen et al., 2023b). Chronic hyperglycemia and low pH conditions (pH 5.5–6.5) in diabetic wounds also create a highly favorable environment for the growth and proliferation of pathogenic bacteria such as *Staphylococcus aureus*, *Pseudomonas aeruginosa*, and *Escherichia coli* (Han et al., 2025). Such bacterial infections further exacerbate the local inflammatory response, increase oxidative stress through excessive ROS production, and significantly impair the critical transition from the inflammatory phase to the proliferative phase in the normal wound healing process (Chen et al., 2023b).

Various innovative strategies have been explored to develop bioactive hydrogel-based wound dressings capable of addressing the complex challenges associated with diabetic wound healing. For instance, an oxidized carrageenan hydrogel modified with dopamine and zinc ions was designed, demonstrating superior antibacterial activity against *E. coli* and *S. aureus*, as well as excellent self-healing ability (Khodaei et al., 2023). Another finding, a multifunctional curcumin-based hydrogel combined with chitosan and sodium alginate was fabricated, exhibiting strong antimicrobial performance, potent antioxidant and anti-inflammatory effects, and enhanced angiogenesis, which collectively accelerated diabetic wound healing in a rat model (Ali et al., 2024). Introduced a nano-in-micro strategy using chitosan-carrageenan microbeads incorporating curcumin-loaded rhamnosomes, achieving highly effective antibacterial activity against multidrug-resistant pathogens and controlled drug release (Ali et al., 2024). Meanwhile, developed an injectable chitosan-carboxymethyl cellulose hydrogel containing nano-curcumin, which demonstrated favorable rheological properties, sustained drug release behavior, and significantly improved diabetic wound closure (Shah et al., 2023).

However, most previous studies have primarily focused on binary material combinations, such as carrageenan–chitosan or chitosan–curcumin, and have not comprehensively explored the potential optimal synergistic effects achieved through the simultaneous integration of all three bioactive components such as carrageenan, chitosan, and curcumin, as a smart responsive material for diabetic wound dressing. Such a tri-component system is expected to create a more integrated therapeutic network: carrageenan contributing to mechanical integrity and moisture retention, chitosan providing inherent antibacterial and hemostatic properties, and curcumin delivering potent antioxidant and anti-inflammatory effects (Madaniyah et al., 2025). The cooperative interactions among these components may enhance physicochemical stability, optimize drug retention and release kinetics, and amplify biological efficacy beyond additive effects. In this work, we prepare and comprehensively characterize the physicochemical properties and biological activities of carrageenan–chitosan–curcumin hydrogel films as stimulus-responsive smart materials for diabetic wound dressing applications.

The study focuses on determining the optimal carrageenan composition through physical performance tests, including swelling capacity, degradability, and mechanical integrity, as well as evaluating antibacterial and antioxidant activities through in vitro assays. The selection of A1–A3 compositions was designed to systematically evaluate the effect of carrageenan concentration as the primary polymer on the physicochemical and functional properties of the hydrogel, while maintaining constant concentrations of chitosan (0.5%) and curcumin (0.05%). The carrageenan levels of 1% (A1), 1.5% (A2), and 2% (A3) represent a gradient of network density from low to high, which directly influences the degree of crosslinking, swelling capacity, mechanical stability, and controlled release behavior of the active compound. This compositional variation was employed to elucidate the structure-property relationships of the hydrogel system and to determine the optimal formulation that achieves a balanced performance in terms of flexibility, water retention, and biological activity for wound dressing applications.

The integration of three biomaterials will provide synergistic therapeutic effects to promote wound healing by ensuring physical protection, regulating inflammation, preventing bacterial infection, reducing oxidative stress, and promoting tissue regeneration. The need of this work arises from multifunctional wound dressings that are responsive to the dynamic microenvironment of diabetic wounds, including fluctuations of pH and glucose levels, and adjust drug delivery and/or material degradation accordingly. Thus, the development of stimulus-responsive hydrogels based on natural biopolymers that are safe, effective, and economically feasible represents a promising strategy to improve clinical outcomes and reduce the substantial economic burden associated with chronic wound complications. Although the hydrogel films were prepared from naturally derived biomaterials with previously reported biocompatibility, detailed cytotoxicity and cell viability evaluations were not included in the present study and should be investigated in future work to further validate their biomedical applicability.

2. EXPERIMENTAL SECTION

2.1 Material and Instrumentations

The materials used in this study include carrageenan obtained from PT. Kappa Carrageenan Nusantara (Pasuruan, East Java, Indonesia; 7.64° S, 112.90° E), chitosan with a molecular weight of 75–80% (sigma aldrich) dissolved in 2% (v/v) glacial acetic acid from Emsure, curcumin extracted from *Curcuma*

longa L, using ethanol 98% (v/v) as the purity was confirmed by LC-HRMS (the extraction method is provided in the supplementary material), 2% PEG 400 as a plasticizer, 1 M KCl as an ionic crosslinker, PBS (pH 7.4), 2,2-Diphenyl-1-picrylhydrazyl (DPPH), and distilled water.

The resulted hydrogel films were characterized by ATR–FTIR spectroscopy (Shimadzu 84000s), FESEM–EDS (FEI Quanta FEG 650 with Oxford Instruments X-act EDS detector), Olympus CX33 stereo microscope equipped with an Olympus EP50 camera. Particle size analysis (CILAS 1090 DRY) was used to investigate particle size of carrageenan TGA.

2.2 Film Hydrogel Preparation

Chitosan powder was dissolved in 2% acetic acid and stirred at 200 rpm until homogeneous. Carrageenan powder was dissolved in distilled water at 80°C and stirred at 200 rpm until homogeneous, followed by the addition of 1 M KCl under continuous stirring at 80°C. The chitosan solution was then added to the carrageenan solution and stirred for 30 min at 200 rpm. The mixture was cooled to 40°C, and curcumin and PEG-400 were added while stirring until fully blended. A total of 15 mL of the solution was cast into a 9 cm Petri dish and dried at room temperature. The dried carrageenan/chitosan/curcumin hydrogel film was peeled off and stored in a desiccator. In this preparation, the carrageenan concentration was varied at 1%, 1.5%, and 2%, while chitosan (0.5%) and curcumin (0.05%) concentrations were kept constant. These formulations were referred to as A1, A2, and A3, respectively, based on their carrageenan content.

2.3 Physical Characteristics

The physical characteristics of the hydrogel films analyzed in this study include film thickness, pH, swelling behavior, moisture content, and degradation. Film thickness was measured using a digital micrometer by cutting the hydrogel film into 2 × 2 cm pieces. Measurements were performed in triplicate (n = 3) to obtain the mean value and standard deviation.

The pH of the hydrogel film was measured using a pH meter. Film samples (2 × 2 cm) were placed into vials containing 10 mL of distilled water and shaken at 100 rpm for 1 h. The pH of the solution was then recorded, and measurements were conducted in triplicate (n = 3) to obtain the mean and standard deviation.

The swelling test was performed by cutting the hydrogel film into (2 × 2) cm pieces and weighing the dry sample to obtain the initial weight (Wo). The film was then immersed in PBS solution (pH 7.4) and incubated for 1, 2, 4, 6, 12, and 24 h. At each time interval, the sample was removed, gently blotted with filter paper without applying pressure, and weighed to obtain the swollen weight (Wt). Measurements were repeated three times (n = 3) to calculate the standard deviation. The swelling percentage was calculated using Equation (1).

$$\text{Swelling ratio (\%)} = \frac{W_t - W_o}{W_o} \times 100\% \quad (1)$$

The moisture content test was carried out by cutting the hydrogel film into (2 × 2) cm pieces and weighing it to obtain the initial weight (W_o). The sample was then dried in an oven at 105°C for 4–6 h until a constant weight was achieved and subsequently weighed again to obtain the final weight (W_t). The measurements were performed in triplicate (n = 3) to obtain the mean and standard deviation. The percentage of moisture content was calculated using Equation (2).

$$\text{Moisture (\%)} = \frac{W_o - W_t}{W_o} \times 100\% \quad (2)$$

The degradation test was performed by cutting the hydrogel film into 2 × 2 cm pieces and weighing it to obtain the initial weight (W_o). The film samples were then immersed in 20 mL of PBS solution (pH 7.4) and incubated at room temperature for 1, 3, 7, and 14 d. After incubation, the films were removed, dried in an oven at 50°C until a constant weight was reached, and then weighed to obtain the final weight (W_t). The measurements were carried out in triplicate (n = 3) to obtain the mean and standard deviation. The degradation percentage was calculated using Equation (3).

$$\text{Degradation (\%)} = \frac{W_o - W_t}{W_o} \times 100\% \quad (3)$$

2.4 Mechanical Characteristics

The mechanical characteristics of the hydrogel films analyzed in this study include tensile strength and elongation at break. The mechanical properties of the carrageenan/chitosan/curcumin hydrogel films were evaluated by measuring tensile strength and elongation at break using a universal testing machine (UTM). Prior to testing, the hydrogel films (A1–A3) were cut into rectangular specimens with dimensions of approximately 10 mm × 50 mm and conditioned at room temperature (25 ± 2°C) and relative humidity of 50 ± 5% for 24 h to ensure uniform moisture distribution. The thickness of each film was measured using a digital micrometer at three different points, and the average value was used for calculation. The specimens were mounted between the grips of the testing machine with an initial gauge length of 30 mm. The test was performed at a constant crosshead speed of 10 mm/min until the film broke. Tensile strength (MPa) was calculated using Equation (4):

$$\text{Tensile strength} = \frac{F_{\max}}{A} \quad (4)$$

where $F_{\max}$ is the maximum force at break (N), and A is the initial cross-sectional area of the film (mm^2). Elongation at break (%) was calculated using Equation (5):

$$\text{Elongation at break} = \frac{L - L_o}{L_o} \times 100\% \quad (5)$$

where L_o is the initial gauge length (mm), and L is the length at break (mm). All measurements were conducted in triplicate (n = 3), and the results were expressed as mean ± standard deviation.

2.5 Chemical Characterization

2.5.1 Particle Size Analyzer

The particle size of carrageenan was analyzed using laser diffraction -based particle size analysis (PSA). A carrageenan sample of 1 g was briefly sonicated for 60 s to minimize agglomeration. Measurements were performed in triplicate, and the particle size distribution was reported as D10, D50, D90, and volume-weighted mean diameter with standard deviation.

2.5.2 ATR-FTIR

The functional group analysis of the hydrogel films was performed using Fourier Transform Infrared Spectroscopy in ATR mode (ATR-FTIR). The carrageenan powder sample and hydrogel film samples (A1, A2, and A3) were placed directly onto the ATR crystal, and the spectra were recorded in the range of 4000–400 cm^{-1}. The spectra were processed using baseline correction and normalization to compare characteristic vibrational bands, such as sulfate, –OH, and –C–O–C, with the structure of carrageenan.

2.5.3 FESEM-EDS

The morphology and composition of the carrageenan and hydrogel films were analyzed using field-emission scanning electron microscopy (FESEM) combined with energy dispersive X-ray spectroscopy (EDS). The samples were mounted on an aluminum stub and coated with a thin layer of Au/Pd (5~ nm) using a sputter coater to prevent charge accumulation. FESEM was operated at an accelerating voltage of 5–15 kV, and images were captured at various magnifications to evaluate the surface morphology and particle distribution. EDS analysis was performed under the same voltage conditions to identify the primary elements and provide semi-quantitative elemental mapping.

2.5.4 Stereo Microscope

The hydrogel films were cut into pieces measuring approximately (0.5 × 0.5) cm using a sterile blade. Thin film samples were mounted on a glass slide, while thicker films were placed directly on the microscope stage. Observations were performed using a 10× objective lens to obtain surface morphology images. Imaging was carried out using an EP50 camera attached to the trinocular port and connected to a computer via the EP view software.

2.6 Thermogravimetric Analysis

The thermal stability of the carrageenan/chitosan/curcumin hydrogel films was evaluated using thermogravimetric analysis (TGA). Approximately 5–10 mg of each dried hydrogel film sample (A1–A3) was placed in a platinum crucible and analyzed using a thermogravimetric analyzer. The measurements were conducted under a nitrogen atmosphere with a constant flow rate of 50 mL/min to prevent oxidative degradation. The samples were heated from 30°C to 600°C at a heating rate of 10°C/min. The weight loss (%) was continuously recorded as a function of temperature to determine the thermal degradation behavior of the hydrogel films. The derivative thermogravimetric (DTG) curves were also obtained to identify the maximum degradation temperature (Tmax) of each decomposition stage. All measurements were performed in triplicate to ensure reproducibility, and the average values were used for analysis. The thermal degradation stages were evaluated based on weight loss regions corresponding to moisture evaporation, polymer decomposition, and carbonization processes.

2.7 *In Vitro* Evaluation of Hydrogel Films

2.7.1 Antibacterial Activity Test

Antibacterial activity was evaluated using the agar well diffusion method on Nutrient Agar (NA) against *Staphylococcus aureus* (Gram-positive) and *Escherichia coli* (Gram-negative). Bacterial cultures were refreshed on NA medium, then the inoculum suspension was prepared in Nutrient Broth and adjusted to a turbidity equivalent to McFarland standard 0.5 (≈ 1×10^8 CFU/mL). A volume of 100 μL of the bacterial suspension was evenly spread over the surface of sterile NA plates using a sterile cotton swab. Wells with a diameter of 6 mm were created using a sterile cork borer and filled with 50 μL of the hydrogel film sample solution at various concentrations.

The plates were incubated upside down at 37°C for 24 h. Antibacterial activity was evaluated by measuring the diameter of the clear zone (inhibition zone) around the wells using a Vernier caliper in millimeters. All experiments were conducted in triplicate, and the results were expressed as the mean ± standard deviation. Antibacterial effectiveness was determined based on the inhibition zone diameter; the larger the inhibition zone, the stronger the antibacterial activity.

2.7.2 Antioxidant Activity Test

Distilled water (3 mL) was pipetted into a test tube and mixed with 1 mL of 0.2 mM DPPH solution. The λ_{max} and absorbance were determined by placing the solution into a cuvette and measuring it using a visible spectrophotometer within the wavelength range of 400–600 nm. Hydrogel film samples at concentrations of 10, 20, 30, 40, and 50 ppm were dissolved in ethanol. A total of 3 mL of each sample solution was pipetted and mixed with 2 mL of 0.2 mM DPPH solution, followed by homogenization using a vortex mixer at room temperature. The mixture was then incubated at 37°C for 30 min, and the absorbance was measured using a visible spectrophotometer at the previously determined maximum wavelength. Absorbance values at each sample concentration were used to calculate the antioxidant activity percentage (%) according to Equation (6).

$$\%\ \text{Antioxidant Activity} = \frac{\text{Control Absorbance} - \text{Sample Absorbance}}{\text{Control Absorbance}} \times 100\% \quad (6)$$

After obtaining the antioxidant inhibition percentage (%), the IC_{50} value of each sample was calculated using linear regression analysis in Microsoft Excel. The regression equation was used to determine the relationship between the hydrogel film concentration and the percentage (%) of antioxidant inhibition. A lower IC_{50} value indicates stronger antioxidant activity.

2.7.3 Percentage Release Curcumin

Hydrogel films (A1–A3) were cut into 2 × 2 cm and immersed in 20 mL PBS (pH 7.4) at 37°C under gentle shaking (100 rpm). At predetermined intervals (1, 2, 4, 6, 12, 24, 48 h), 2 mL aliquots were withdrawn and replaced with fresh PBS. The released curcumin concentration was analyzed using UV–Vis spectrophotometry at $\lambda_{max} \approx 425$ nm. All measurements were performed in triplicate. The cumulative release of curcumin was calculated based on the concentration obtained from UV–Vis analysis using a calibration curve. The percentage of release was determined by comparing the cumulative amount of released curcumin to the total drug content in the hydrogel. The cumulative percentage of curcumin release was calculated using Equation (7).

$$\% \text{ Release Curcumin} = \frac{C_t \times V}{M_o} \times 100\% \quad (7)$$

where C_t is the concentration of curcumin at time t, V is the release medium volume, and M_o is the initial amount of curcumin loaded in the hydrogel.

2.8 Analytical Statistic

All experiments were performed in triplicate ($n = 3$). Statistical analysis was conducted using one-way analysis of variance (ANOVA) at a significance level of $p < 0.05$, followed by Duncan's multiple range test, using IBM SPSS Statistics (version 25.0; IBM, Armonk, NY, USA). Significant differences among groups are indicated by different superscript letters.

3. RESULTS AND DISCUSSION

3.1 Carrageenan characterization

The smart behavior of carrageenan as a sustainable material is governed by the interrelationship between particle size, chemical structure, and microstructural morphology. Through integrated characterization using particle size analysis (PSA), ATR-FTIR, and FESEM-EDS, this study elucidates how these parameters collectively support the formation of adaptive hydrogel systems.

Particle size analysis revealed that carrageenan exhibits a broad size distribution, with a median particle size (D_{50}) of 124.11 μm and an average particle size of 140.38 μm (Figure 1a). This indicates the predominance of medium-to-large particles. Although larger particles generally require longer hydration times, once fully dissolved they promote the formation of a more porous hydrogel network. Such porosity is beneficial because it enhances water absorption capacity and facilitates mass transport within the hydrogel matrix, which are essential characteristics of sustainable smart materials (Atgié et al., 2019; Chen et al., 2018).

The FTIR spectrum of carrageenan shows characteristic absorption bands of sulfated polysaccharides. The broad band at 3381.55 cm^{-1} corresponds to –OH stretching vibrations, indicating a highly hydrophilic structure with extensive hydrogen bonding that supports swelling and gel matrix formation (Necas and Bartosikova, 2013; Vilchez et al., 2021). The band at 1635.86 cm^{-1} is attributed to C=O stretching or bound water, suggesting a stable polymer network with preserved helical structure (Figure 1b).

The absorption at 1370.59 cm^{-1} is associated with C–H stretching or CH_2 deformation of the galactose backbone, confirming the β-1,4 and α-1,3 glycosidic linkages of carrageenan. The strong band at 1223.69 cm^{-1} corresponds to the asymmetric stretching of sulfate ($-SO_3^-$) groups, serving as a key indicator of κ-carrageenan (Rupert et al., 2022). The sulfate substitution at the C-4 position of galactose is further confirmed by the band at 840 cm^{-1}, which underlines the anionic polyelectrolyte nature of carrageenan and its ability to form ionic interactions with chitosan (Hidayaty et al., 2026). Additionally, the band at 922 cm^{-1} indicates the presence of 3,6-anhydrogalactose, confirming double-helix formation as the basis of gelation. Overall, these functional groups confirm the ability of carrageenan to form a three-dimensional hydrogel network, interact electrostatically with chitosan, and encapsulate curcumin, supporting its application as a smart material for diabetic wound dressing systems.

Figure 1c shows FESEM–EDS analysis to assess the morphological and elemental characteristics of carrageenan powder. FESEM images show a heterogeneous lamellar morphology with fibrous fragments, indicating that the polysaccharide is dispersed as irregular flakes. BSE/SE imaging at 60× magnification (500 μm scale) demonstrates that the material consists mainly of thin lamellar fragments with fibrous edges and smaller particles occupying interlayer spaces, resulting in a rough surface associated with aggregated polysaccharide chains. The presence of localized fine-particle clusters suggests a broad particle size distribution, including partially dispersed micro–nano fractions (Campo et al., 2009; Necas and Bartosikova, 2013).

EDS analysis (Figure 1c) confirms that carbon (52.75%) and oxygen (34.53%) are the dominant elements, consistent with a polysaccharide matrix. The sulfur content (5.50%) verifies the presence of sulfate groups ($-OSO_3^-$) characteristic of κ-carrageenan, which are critical for gelation behavior and hydrophilicity. Potassium ions (6.18%) contribute to gel network stabilization, while trace elements such as Cl, Na, and Mg likely originate from residual salts or marine minerals.

Overall, the lamellar and fibrous morphology supports the formation of double-helix structures and ionic interconnections during hydration, leading to a porous hydrogel matrix with high swelling capacity and controlled bioactive release. These morphological features collectively govern swelling behavior and drug-release kinetics, confirming the suitability of

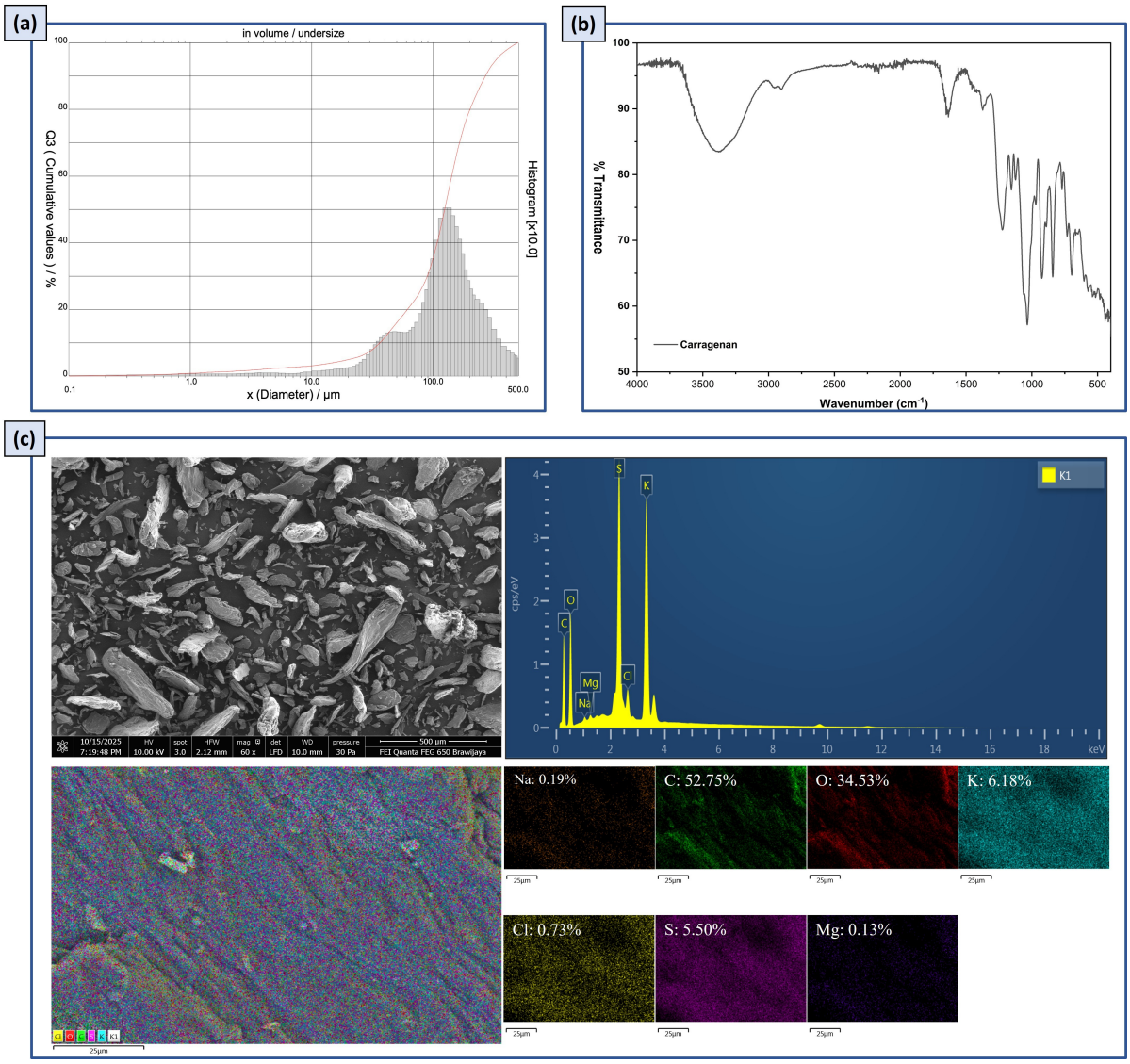

Figure 1. Characterization of Carrageenan: Particle Size Analyzer (PSA) (a), FTIR Spectra (b), and FESEM EDX Analyzer (c)

carrageenan as a smart hydrogel-forming material.

3.2 Physical Characteristics of Film Hydrogel

The physical properties of the carrageenan/chitosan/curcumin hydrogel films prepared using A1–A3 formulation were evaluated to study crucial performance parameters of wound dressing, such as film thickness, surface pH, swelling capacity, moisture content, and hydrogel degradation rate. Differences in carrageenan concentration in the formulations lead to different physical properties influenced by variation in polymer matrix density, water-retention capacity, and surface structural stability.

This assessment underlies establishing the film's application to a moist, stable, and biocompatible wound healing microenvironment for diabetics. Overall, all formulations exhibited physical values within the acceptable range for wound dressing materials, with characteristic differences that highlight the influence of carrageenan concentration on hydrogel structure and functionality. The physical characteristics of the hydrogel films are presented in Table 1, and their visual morphology is shown in Figure 2.

The physical attributes of the carrageenan/chitosan/curcumin hydrogel films were determined with adherence to the following three parameters: film thickness, moisture content, and film pH. The three formulations, A1–A3, possessed different concentrations of carrageenan (1%, 1.5%, and 2%), while the concentrations of chitosan (0.5%) and curcumin (0.05%) were kept constant. Therefore, the differences in physical performance are mainly attributed to the variation in carrageenan content as the key structural polymer. Overall, all formulations remained within the recommended physical property range for wound-dressing hydrogel films (Boateng et al., 2008; Szliszka

Table 1. Physical Characteristics of Hydrogel Film Formulations (A1–A3)

Parameter	A1	A2	A3	Standard
Film thickness (mm)	0.10 ± 0.001	0.20 ± 0.001	0.30 ± 0.002	0.05–0.30
Moisture content (%)	10.72 ± 0.22	20.63 ± 0.49	20.95 ± 0.81	10.00–30.00
Film pH	5.50 ± 0.35	6.23 ± 0.31	6.00 ± 0.50	5.5–6.5

et al., 2009).

The increase in film thickness from A1 to A3 (Table 1) demonstrates a linear relationship between carrageenan concentration and polymer network density. Higher carrageenan content enhances double-helix formation and ionic crosslinking between sulfate groups and K^+ ions, resulting in a more compact and mechanically strengthened matrix (Amine et al., 2019). The maximum thickness observed in A3 suggests a stronger crosslinked network, although it may reduce film flexibility and induce particle agglomeration.

In contrast, moisture content exhibited a different trend. A1 showed the lowest moisture level due to the reduced capacity of its less concentrated polymer network to retain water. Meanwhile, A2 and A3 presented nearly double the moisture content, consistent with the hydrophilic behavior of sulfated groups ($-OSO_3^-$), which readily bind water molecules via hydrogen bonding (Necas and Bartosikova, 2013). The moisture content range of 20–21% falls within the optimal zone for wound dressing materials, sustaining a moist healing environment without causing tissue maceration (Brett, 2006).

The pH values of the hydrogel films fall within the physiological range of healthy skin (Table 1). Maintaining an appropriate pH prevents irritation and supports the optimal antibacterial activity of chitosan, which occurs in mildly acidic conditions ($pH < 6.5$). The differences in pH were attributed to the carrageenan content and carrageenan's interaction with chitosan, where higher concentrations of carrageenan provide a stronger buffering capacity toward chitosan ammonium ions ($-NH_3^+$) Rinaudo (2006).

Regarding the physical characteristics of the films (Table 1 and Figure 2), it was found that increasing the carrageenan concentration from 1% to 2% clearly influenced thickness, water content, and surface homogeneity. The A1 formulation showed the lowest film thickness with low moisture content, indicating a loose material structure and poor water-storage capacity. The A2 formulation exhibited the most balanced characteristics, with optimal thickness and moisture content, pH values close to physiological skin conditions, stable polyelectrolyte interactions, and acceptable water permeability. On the other hand, formulation A3, containing the highest carrageenan concentration, produced the thickest film with the highest water retention but also showed surface aggregation, which may reduce flexibility and limit drug diffusion.

Overall, the results demonstrate that increasing the carrageenan ratio enhances water-retention capacity and structural stability, whereas formulation A2 provides the optimal compromise between mechanical strength, moisture condition, and physiological pH compatibility. This finding is consistent with theories regarding carrageenan–chitosan polyelectrolyte hydrogel formation, where increased carrageenan concentration promotes enhanced double-helix formation and K^+-mediated ionic crosslinking, leading to the formation of more compact and mechanically reliable film structures (Amine et al., 2019). Electrostatic attraction between carrageenan sulfate groups ($-SO_4^-$) and chitosan ammonium groups ($-NH_3^+$) also contributes to the formation of a strong and continuous hydrogel network (Chen et al., 2018). In formulation A2, the optimal crosslink density and matrix porosity facilitate maximum water retention and flexibility (Boateng et al., 2008). Curcumin remains stable under mildly acidic conditions and interacts with the hydrogel network through hydrogen bonding (Priyadarsini, 2014).

Therefore, the formulation containing 1.5% carrageenan (A2) provides the most suitable performance for diabetic wound dressing applications due to its simultaneous fulfillment of moisture, structural stability, and skin-compatibility requirements.

Another critical physical characteristic of hydrogel films is their ability to absorb exudate, expressed as swelling percentage. The swelling analysis of formulations A1–A3 demonstrated contrasting hydration behavior depending on differences in carrageenan concentration within the polymer matrix. Although swelling increased with longer immersion time for all formulations, the absorption characteristics were strongly influenced by hydrophilic charge density, degree of ionic crosslinking, and flexibility of the carrageenan–chitosan polyelectrolyte structure.

The high carrageenan content of A3 resulted in rapid initial swelling due to the greater availability of hydrophilic groups. In contrast, formulation A2 exhibited a gradual swelling pattern and reached its maximum swelling capacity after 24 h, reflecting a more stable and controlled network structure. Formulation A1 showed a continuous and moderate swelling pattern throughout immersion. These differences suggest structural variations within the hydrogel matrix that may influence the diffusion and retention capacity of PBS ions as well as water uptake. The swelling profiles of the three formulations are presented in Figure 3.

Based on Figure 3, the water absorption capacity of the hydrogel films was strongly influenced by carrageenan concentration. Formulation A3 (2% carrageenan) exhibited the highest swelling during the early-to-mid testing phase due to its high density of negatively charged sulfate groups ($-SO_3^-$), which facilitated extensive PBS uptake through osmotic swelling. However, the swelling rate gradually decreased during the later

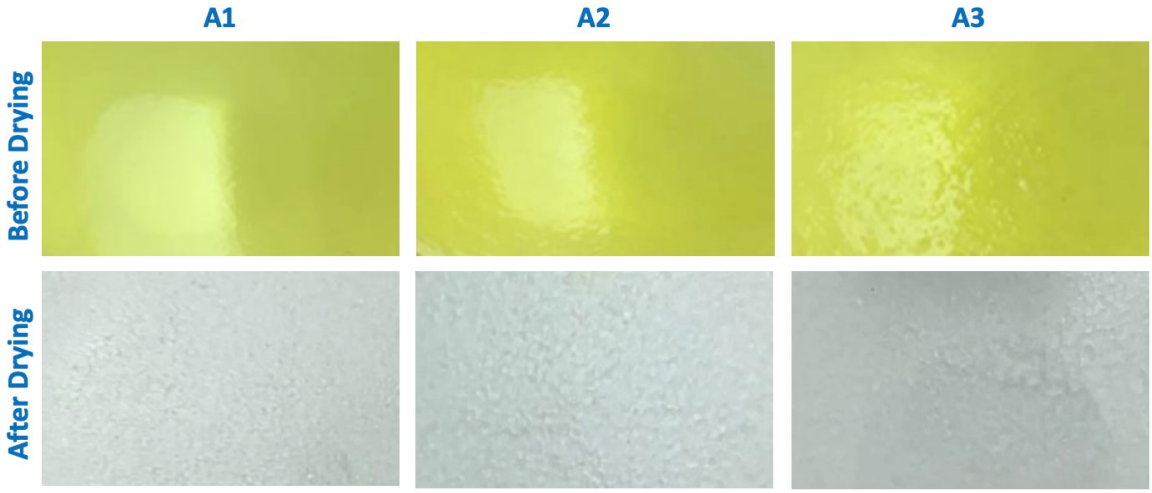

Figure 2. Stereo Microscopy Images of Hydrogel Films A1–A3 Before and After the Drying Process

phase, likely due to the formation of a denser polymeric network caused by KCl-mediated crosslinking, which restricted further expansion.

In contrast, formulation A2 (1.5% carrageenan) demonstrated a gradual increase and reached the highest swelling capacity after 24 h. This delayed-swelling behavior suggests a more optimal network density, allowing progressive chain relaxation until maximum expansion was achieved. Formulation A1 (1% carrageenan) displayed moderate and relatively stable swelling behavior, indicating a low-density network that rapidly reached equilibrium but could not retain PBS as effectively as A2 and A3.

These findings indicate that increasing carrageenan concentration does not produce a linear response in swelling performance. The swelling behavior of polyelectrolyte hydrogels is governed by charge density, crosslinking degree, and chain flexibility (Hoare and Kohane, 2008). Carrageenan, as an anionic polymer containing hydrophilic sulfate groups, strongly attracts water molecules, while chitosan forms polyelectrolyte complexes through electrostatic interactions (Ahmed, 2015; Szliszka et al., 2009). Among the formulations, A2 provided the best balance between network flexibility and charge density, resulting in superior late-stage PBS absorption, making it a promising candidate for hydrogel wound dressings requiring prolonged hydration.

Degradation analysis was performed to evaluate the structural stability of the hydrogel films in PBS. Higher carrageenan concentrations resulted in denser polymer matrices that degraded more slowly, whereas lower carrageenan concentrations accelerated the degradation process. This behavior is important in selecting the optimal formulation because degradation characteristics directly influence moisture-retention ability and the expected duration of wound-dressing application. The degradation profiles of formulations A1–A3 are presented in Figure 4.

The degradation study of hydrogel films in PBS medium (pH = 7.4) was conducted to analyze the structural stability and degradation rate of the hydrogel films under physiological conditions. This parameter is essential because hydrogel-based wound dressings should maintain sufficient physical integrity while gradually degrading in response to wound-exudate dynamics. Formulations A1 (1% carrageenan), A2 (1.5%), and A3 (2%), combined with chitosan (0.5%) and curcumin (0.05%), were evaluated over 1, 3, 7, and 14 d. The results indicated significant differences in degradation rates among the formulations, mainly attributed to carrageenan concentration.

These differences correlate strongly with the density of the hydrogel network. Carrageenan, an anionic polymer, forms gel structures through double-helix associations and ionic crosslinking with cations such as K^+. At higher concentrations (A3), carrageenan produces a denser polymeric matrix that slows water penetration and enhances resistance to structural disintegration. Conversely, the lower carrageenan concentration in A1 results in a looser network that is more susceptible to fragmentation. Since the chitosan concentration remained constant across all formulations, the variations in degradation behavior were primarily governed by carrageenan content.

The degradation profile demonstrated that A1 exhibited the highest degradation rate at all observation times, reflecting a porous and less compact network structure. In contrast, A2 displayed moderate structural stability, while A3 exhibited the lowest degradation rate, indicating the formation of the most compact hydrogel network. Therefore, A3 may serve as a suitable candidate for long-term moisture-retention wound dressings, whereas A1 may be more appropriate for wound dressings requiring frequent replacement. Curcumin and chitosan contributed minimally to degradation differences because their concentrations were maintained constant in all formula-

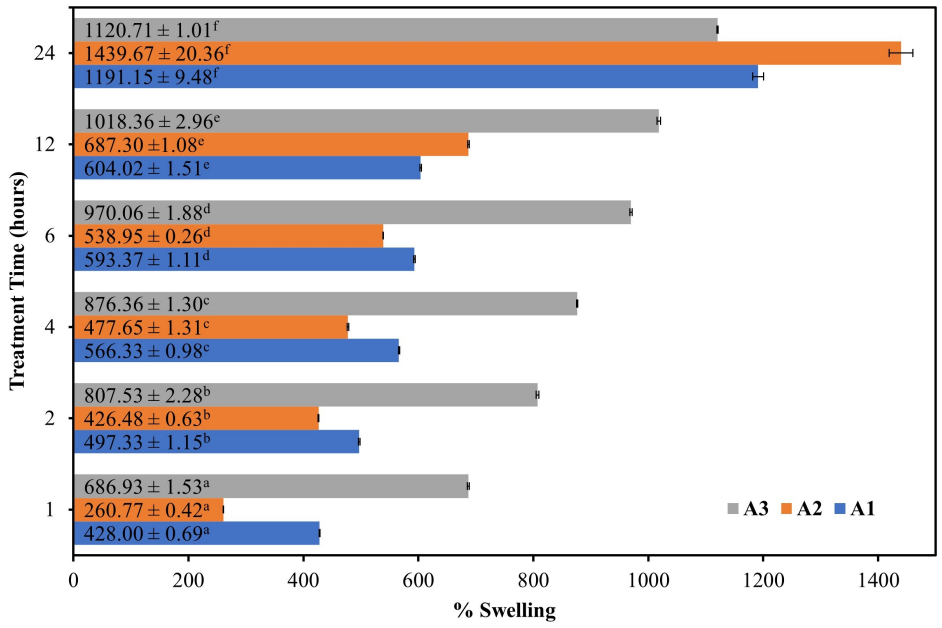

Figure 3. Swelling Percentage of Hydrogel Film Formulations A1–A3

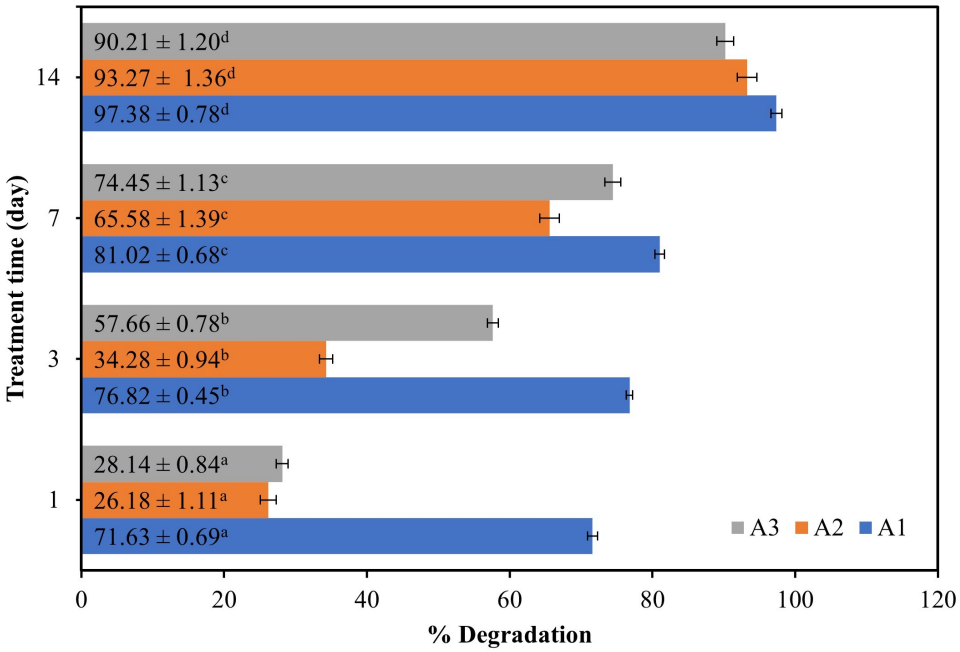

Figure 4. Degradation Capacity of Hydrogel Film Formulations A1–A3

tions.

Overall, these results are consistent with hydrogel polymer theory, where degradation behavior is strongly influenced by polymer composition, crosslinking degree, water absorption capacity, and polymer–solvent interactions. Higher carrageenan concentrations promote the formation of denser hydrogel networks and consequently reduce degradation rates (Necas and Bartosikova, 2013; Rinaudo, 2006; Vilchez et al., 2021). Therefore, hydrogel stability can be optimized through appropriate regulation of carrageenan concentration, enabling the design of wound dressings suitable for chronic wound applications such as diabetic ulcers.

3.3 Mechanical Characteristics of Hydrogel Films

The mechanical properties of carrageenan/chitosan/curcumin hydrogel films prepared using formulations A1–A3 were evaluated to investigate critical wound-dressing performance parameters, including tensile strength and elongation at break. Mechanical characteristics are essential for determining the suitability of hydrogel films as wound dressings, particularly regarding flexibility, durability, and resistance to mechanical stress during application and removal. Therefore, tensile strength and elongation at break were systematically evaluated for formulations A1–A3.

The obtained mechanical properties fall within the acceptable range for hydrogel-based wound dressings. The mechanical characteristics of the hydrogel films are presented in Table 2.

The results demonstrate that carrageenan concentration significantly influences the mechanical behavior of the hydrogel films (Table 2). The tensile strength increased progressively from A1 to A3, indicating that higher carrageenan content enhances the structural integrity of the polymer network. This behavior is attributed to the increased formation of double-helix structures and stronger ionic interactions between carrageenan sulfate groups ($-SO_4^-$) and chitosan ammonium groups ($-NH_3^+$), resulting in a more compact and rigid matrix, as reported in previous studies (Campo et al., 2009; Necas and Bartosikova, 2013).

In contrast, elongation at break exhibited the opposite trend, where formulation A1 demonstrated the highest flexibility, whereas A3 showed the lowest elongation value. This finding suggests that increasing carrageenan concentration restricts polymer-chain mobility, thereby promoting the formation of a more brittle network structure (Liu et al., 2023; Rinaudo, 2006). Notably, formulation A2 demonstrated the most favorable mechanical performance, achieving a balanced combination of tensile strength and flexibility. Such balance is critically important for wound-dressing applications because the material must possess sufficient mechanical integrity to maintain its structure while remaining flexible enough to conform to the wound surface without causing discomfort or disrupting newly regenerated tissue (Ahmed, 2015; Boateng et al., 2008).

These findings further confirm that formulation A2 provides an optimal compromise between mechanical strength and elasticity, supporting its potential as an effective hydrogel-based wound dressing.

3.4 Chemical Characteristics of Hydrogel Films

3.4.1 Functional Group Analysis

The chemical characterization results of carrageenan/chitosan/curcumin-based hydrogel films obtained using ATR–FTIR revealed notable spectral changes, indicating significant interactions among the functional groups involved in the formation of the composite hydrogel network for formulations A1–A3. The FTIR spectra showed broadening of the O–H stretching band, variations in intensity and position of characteristic sulfate peaks from carrageenan, and the appearance of amide and aromatic vibration bands. These spectral characteristics indicate the existence of electrostatic interactions and hydrogen bonding between carrageenan and chitosan, as well as the successful incorporation of curcumin into the polymer matrix. These findings confirm the successful formation of a chemically integrated and homogeneous composite hydrogel structure, as presented in Figure 5.

ATR–FTIR analysis of carrageenan/chitosan/curcumin-based hydrogel films was conducted to identify functional-group changes and chemical interactions occurring during the formation of the crosslinked polymer matrix. Based on Figure 5, all spectra exhibit relatively similar transmittance patterns. However, comparison between pure carrageenan and formulations A1–A3 revealed peak shifts, intensity variations, and overlapping peaks, indicating electrostatic interactions, hydrogen-bond formation, and compatibility among the hydrogel components within the film matrix. Variations in carrageenan concentration (A1 = 1%; A2 = 1.5%; A3 = 2%), while maintaining constant amounts of chitosan (0.5%) and curcumin (0.05%), generated spectral patterns reflecting the dominant contribution of carrageenan to sulfate-group intensity and repeating galactose units, together with contributions from chitosan amine groups and curcumin aromatic groups.

The FTIR spectrum of pure carrageenan shown in the reference graph displays distinct characteristic peaks, including O–H stretching vibrations at 3400–3450 cm^{-1}, C–H vibration at 2920 cm^{-1}, sulfate ester (S=O) peak around 1220–1250 cm^{-1}, galactose-4-sulfate peak at 845 cm^{-1}, and the 3,6-anhydrogalactose vibration at 930 cm^{-1}. These four peaks represent the main structural markers of κ-carrageenan as reported in the literature (Rupert et al., 2022; Vilchez et al., 2021). When compared with films A1–A3, these peaks remain visible but exhibit weakened intensity, broadening, or slight shifts. This indicates that although the fundamental structure of carrageenan remains intact, chemical interactions occur with chitosan and curcumin within the film matrix.

In the spectra of A1–A3 (Figure 5), the region of 3600–3000 cm^{-1} shows a broad O–H stretching band, indicating an intensive network of hydrogen bonding among carrageenan chains, chitosan, and curcumin phenolic groups. The O–H band in A3 appears slightly more intense and broader compared to A1 and A2, demonstrating that the higher carrageenan concentration increases the density of hydrogen bonds and the hydration of the matrix. Compared with pure carrageenan, this band shows a slight shift to lower frequencies (~3340–3360 cm^{-1}), which indicates the presence of H-bonding interactions between –OH groups of carrageenan, –OH of curcumin, and $-NH_2$ groups of chitosan protonated in an acidic medium (Aranaz et al., 2021; Rinaudo, 2006).

In the region of 1650–1560 cm^{-1}, peaks associated with amide I and amide II vibrations of chitosan are observed. Although the peak intensity is not dominant, it is still clearly detected, indicating the contribution of chitosan to the film structure. The presence of more pronounced amide bands in A1 suggests that at lower carrageenan concentrations, the amine

Table 2. Mechanical Characteristics of Hydrogel Film Formulations (A1–A3)

Parameter	A1	A2	A3	Standard
Tensile strength (MPa)	0.85 ± 0.07	1.42 ± 0.09	1.95 ± 0.11	0.5–2.5
Elongation at break (%)	68.4 ± 3.2	52.7 ± 2.8	34.9 ± 2.5	30–100

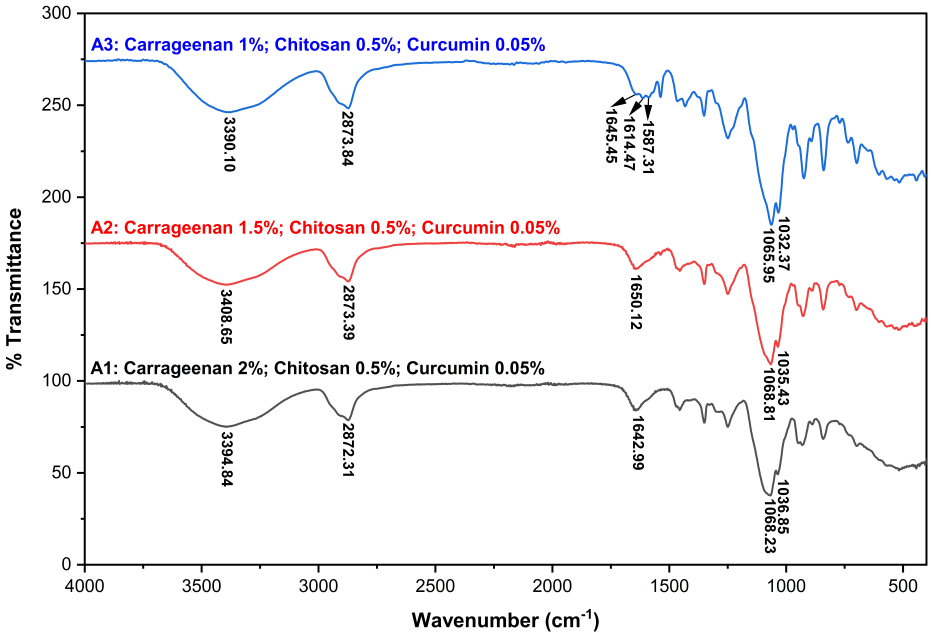

Figure 5. ATR-FTIR Spectra of Hydrogel Film Formulations A1–A3

groups of chitosan are not fully bound to the sulfate groups of carrageenan, whereas in A3 these bands weaken due to stronger electrostatic interactions between $-NH_3^+$ of chitosan and $-SO_4^-$ of carrageenan, forming a more stable polyelectrolyte complex (Atgié et al., 2019; Escárcega-Galaz et al., 2018). This is consistent with the observation that increasing carrageenan dosage reinforces ionic interactions and reduces the vibrational freedom of amine groups.

The region of 1510–1420 cm^{-1} shows shoulders and small peaks characteristic of the aromatic ring of curcumin. Although the intensity is low due to the curcumin concentration being only 0.05%, its presence can still be observed, particularly in A1 and A2. In A3, this peak becomes more merged with the carrageenan bands, indicating stronger hydrogen bonding and potential vibrational shielding effects due to increased matrix density. This is consistent with Priyadarsini (2014), who reported that interactions between curcumin and hydrophilic polymers may reduce the intensity of aromatic peaks due to changes in the electronic environment.

In the fingerprint region (1200–800 cm^{-1}), the three film formulations exhibit significant changes. The sharp characteristic S=O band of carrageenan at 1220–1250 cm^{-1} becomes softened and broadened in all film formulations, particularly in A1. In A3, this peak appears stronger and more defined, reflecting the more dominant proportion of carrageenan within the matrix. The shift of this peak toward lower frequencies (around 1210 cm^{-1}) in A1–A2 indicates the involvement of sulfate groups in ionic complexation with protonated chitosan, a common phenomenon during the formation of polyelectrolyte complexes (PEC) (Atgié et al., 2019; Chen et al., 2018). A similar trend is observed at 845 cm^{-1}, where the C–O–S sulfate vibration shows reduced relative intensity after formulation, confirming the presence of intermolecular interactions.

The peak at 930 cm^{-1} (3,6-anhydrogalactose) remains clearly detectable in all formulations, indicating that the fundamental structure of carrageenan is not degraded during heating and mixing. Its intensity is higher in A2 and A3, consistent with the increased amount of carrageenan. Meanwhile, the C–O–C peak at approximately 1070–1110 cm^{-1} shows increased intensity and band broadening in the A3 film, indicating the formation of a denser hydrogel network and a higher degree of physical crosslinking. This phenomenon has also been reported in other carrageenan–chitosan hydrogels, where broadening of the C–O–C band is considered an indicator of increased network density (Tashakkorian et al., 2020).

The ATR–FTIR spectra show a consistent trend: the higher

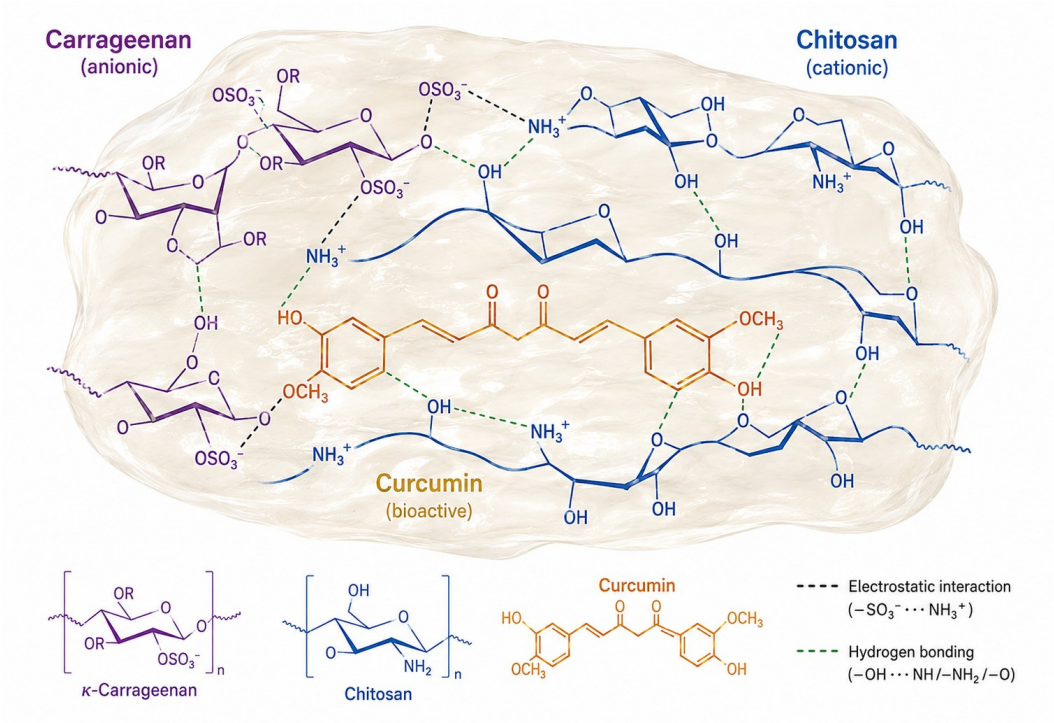

Figure 6. Mechanistic Reaction Illustration Between Carrageenan, Chitosan, and Curcumin

the carrageenan concentration, the stronger the ionic and hydrogen -bond interactions that occur, resulting in more merged functional group peaks and slight spectral shifts. Formulation A1 (1% carrageenan) displays more distinct peak intensities; A2 exhibits a transitional pattern, while A3 presents the most compact and integrated spectrum, consistent with the formation of the densest hydrogel network. The ATR–FTIR analysis indicates that the three hydrogel film formulations A1–A3 successfully formed a stable composite matrix through electrostatic interactions between $-SO_4^-$ groups of carrageenan and $-NH_3^+$ groups of chitosan, as well as hydrogen bonding involving –OH of carrageenan, –OH/–OCH_3 of curcumin, and $-NH_2$ of chitosan (Figure 6). The presence of curcumin is confirmed by the aromatic bands, although their intensity is low due to the small dosage, yet they still demonstrate incorporation within the matrix. Increasing carrageenan concentration results in more integrated peaks, reinforcing the indication of a denser PEC network. FTIR thus confirms that the three components interact within a composite structure rather than merely forming a physical mixture, and A3 provides the strongest evidence of cohesive hydrogel network formation (Lupa et al., 2022).

Carrageenan acts as an anionic polymer providing sulfate groups for ionic interactions; chitosan functions as a cationic polymer supplying protonated amine groups in acidic media; while curcumin serves as a bioactive agent interacting through hydrogen bonding. The electrostatic complexation between carrageenan and chitosan forms a polyelectrolyte network that strengthens the film structure, while curcumin becomes entrapped within the matrix through stabilizing non-covalent interactions. The peak shifts and broadened FTIR bands in all three formulations support the formation of an interpenetrating polymer network, consistent with natural polymer hydrogel theory and the curcumin-binding mechanism in hydrophilic systems. Therefore, ATR–FTIR confirms the chemical compatibility of the three components and the relevance of the formulation as a stable smart-material system for diabetic wound dressing applications.

3.4.2 Morphology and Elemental Mapping Analysis

Chemical characterization of the hydrogel film formulations A1–A3 using FESEM–EDS was conducted to evaluate the surface morphology and elemental composition, which reflect the quality of the polymer matrix formation of carrageenan –chitosan–curcumin at different formulation ratios. FESEM analysis reveals the topography and structural homogeneity of the hydrogel network, while EDS helps identify the distribution of key elements (e.g. C, O, S, Cl, Na, and K) with respect to biopolymer and ionic crosslinker presence. The density, surface regularity, and elemental distribution depend on the concentration of carrageenan and influence the stability of polyelectrolyte interactions and the incorporation of curcumin in the matrix. This analysis provides preliminary understanding of the chemical structure quality and uniformity of the films formed in each formulation, as shown in Figure 7.

FESEM–EDS analysis of hydrogel films for formulations A1, A2, and A3 revealed differences in surface morphology and elemental distribution that reflect variations in the ratios

of carrageenan, chitosan, and curcumin in each formulation. In formulation A1 (1% carrageenan, 0.5% chitosan, 0.05% curcumin), the FESEM images show a relatively heterogeneous surface characterized by regions of material aggregation and amorphous zones distributed unevenly. The surface texture appears less compact with several micro-gaps, indicating that the lower carrageenan content results in a hydrogel network that is insufficiently crosslinked, reducing the strength of intermolecular bonding. Elemental distribution obtained from EDS shows dominance of carbon (C) and oxygen (O), which is typical of biopolymers, along with the presence of sodium (Na), sulfur (S), and chlorine (Cl), originating from the sulfate groups of carrageenan and residual ions from the preparation process. Potassium (K) is also detected in moderate amounts, consistent with the use of KCl as an ionic crosslinker during gel formation. Elemental mapping in A1 demonstrates a relatively uniform distribution of C and O, whereas S and Cl appear localized in specific regions, suggesting heterogeneous interactions between carrageenan and chitosan due to incomplete matrix densification (Campo et al., 2009).

For formulation A2 (1.5% carrageenan), the FESEM images show a more homogeneous and denser surface compared to A1. Thin layered structures appear more regularly arranged, with smaller pore spacing and improved surface continuity. This structural improvement indicates enhanced hydrogel network strength due to increased carrageenan content, promoting double-helix formation and gel aggregation (Reig-Vano et al., 2021; Rinaudo, 2006). Compositional EDS shows an increase in carbon to 62.75%, correlating with the increased polymer matrix density. Sodium remains low (0.44%), while sulfur and chlorine are present at stable concentrations, indicating that the polyelectrolyte system between carrageenan and chitosan is more uniformly established at this ratio. Elemental mapping demonstrates more homogeneous distribution of C, O, S, and Cl, with sulfur–representing sulfate groups of carrageenan–appearing more fully integrated into the network. This suggests that the polymer ratio in A2 supports more stable physical integration, producing a surface with more consistent topography, increased compactness, and reduced curcumin aggregation.

Formulation A3 (2% carrageenan) exhibits the most significant morphological changes. The FESEM images display a much denser surface, approaching a compact block-like or granular structure with larger aggregate clusters. At higher magnification, local crystallinity or dense domains can be observed, formed as a result of the high carrageenan concentration promoting excessive double-helix formation and inter-helix aggregation. Although the structure appears more solid, some regions show uneven surface texture, indicating that excessively high carrageenan content can reduce flexibility and compromise the homogeneity of the hydrogel network. EDS data informs an elemental character still predominated by C and O, with remaining ions Na, S, Cl, and K present at levels comparable to those in A1–A2. However, elemental mapping indicated a higher density of S- and Cl-rich regions associated with carrageenan, corresponding to a more compact carrageenan gel network (although less homogeneous than in A2). This irregularity may arise from excessive crosslinking that impedes an even diffusion of curcumin and chitosan into the matrix.

Morphological and chemical composition analysis through FESEM–EDS shows that the density, homogeneity, and structural integrity of the hydrogel film are significantly affected as the carrageenan content increases from A1 to A3. Formulation A1 shows a less compact surface and a very diverse elemental distribution, while A2 has the best stability, homogeneity, and distribution, providing the best polymer ratio for the hydrogel matrix formation. Formulation A3 produces a highly dense but less uniform structure, suggesting the occurrence of carrageenan crosslinking saturation. Therefore, empirically, A2 demonstrates the best suitability for wound dressing applications as it provides a combination of homogeneous structure, more uniform curcumin distribution, and the most stable polyelectrolyte interaction. These findings are consistent with the theory that an ideal hydrogel network should possess uniform micro-porosity, a surface that is not overly dense, and evenly distributed elements to maintain moisture, allow oxygen diffusion, and support controlled drug release (Atgié et al., 2019; Szliszka et al., 2009). Hence, according to experimental evidence, the highest performance in controlling porosity, chemical stability, and biological interaction effect on diabetic wound dressing could be attributed to the A2 formulation.

Quantitative pore size or porosity distribution analysis was not conducted because the carrageenan/chitosan/curcumin hydrogel films are composed of natural polymeric materials with fragile hydrated structures that are highly susceptible to deformation during conventional porosity characterization procedures involving vacuum, degassing, or gas adsorption treatment. Such conditions may alter the native morphology of the hydrogel network and produce non-representative pore characteristics. Therefore, FESEM analysis in this study was focused on qualitative observation of surface morphology and structural compactness of the hydrogel matrix.

3.4.3 3D Morphology Analysis

Hydrogel films of A1–A3 formulations were examined microscopically with an Olympus CX33 microscope combined with an EP50 camera after five months of storage to capture the stability of the surface (surface stability, matrix homogeneity, and potential biological changes during storage). In general, comparisons of those micrographs indicated differences in the structural density and smoothness of the formulations; however, there was no morphological evidence of microbial growth or biological degradation. Variations in appearance among the formulations were primarily related to the carrageenan composition, which influences gel network density, whereas the surface characteristics remained stable without the presence of foreign structures such as bacterial colonies. The three-dimensional morphology, structural stability, and biological evaluation of hydrogel films A1–A3 are presented in Figure 8.

Microscopic observations using an Olympus CX33 microscope combined with an Olympus EP50 digital camera en-

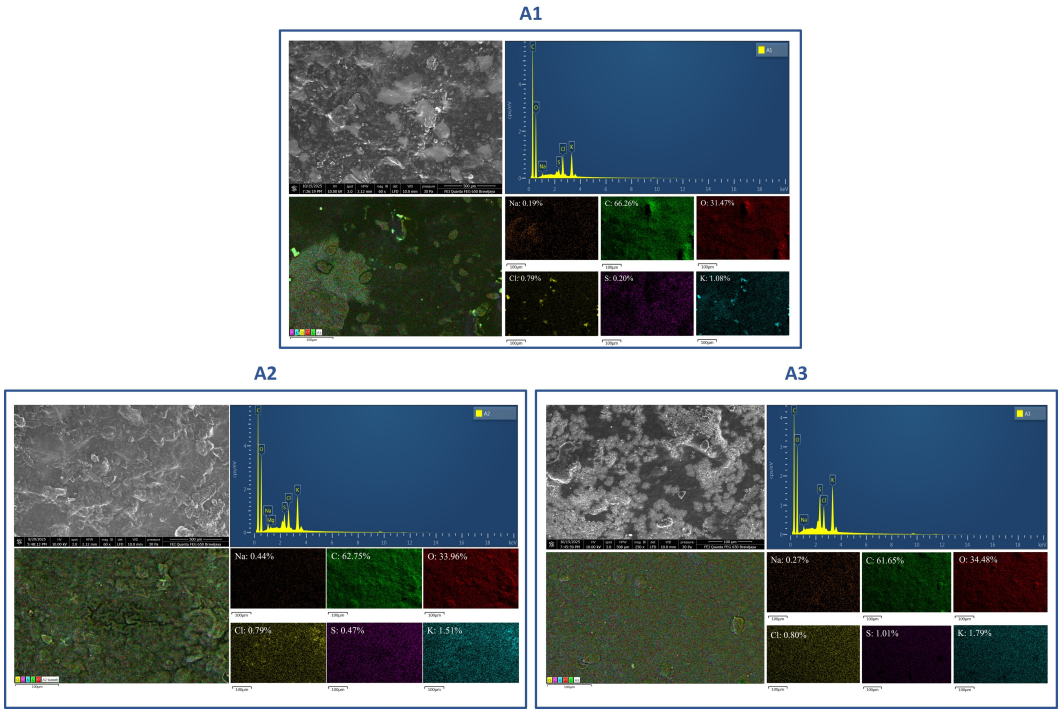

Figure 7. FESEM–EDS Morphology of Hydrogel Films

abled clear visualization of the surface structure of carrageenan–chitosan–curcumin hydrogel films at 10× magnification. Images of formulations A1, A2, and A3 reveal significant differences in matrix density, pore distribution, and surface homogeneity, closely related to the variation in carrageenan concentration (1%, 1.5%, and 2%). In formulation A1, the surface appears highly porous, rough, and heterogeneous, with large cavities and dark regions indicating non-uniform polymer network formation, consistent with the low carrageenan concentration that is insufficient to form a stable gel network. The enlarged image shows a hollow, irregular pore structure, demonstrating a loosely compacted hydrogel matrix. Biologically, such morphology tends to be more vulnerable to the intrusion of foreign particles; however, no bacterial growth was observed.

Unlike A1, the A2 film exhibits a more compact, homogeneous structure with fine porosity, reflecting more optimal polyelectrolyte interactions between carrageenan and chitosan (Tian et al., 2019). The smoother surface and smaller pore distribution indicate the formation of a more stable three-dimensional hydrogel network. The magnified image shows tighter polymer aggregation, absence of large dark regions, and reduced surface roughness. This pattern suggests a well-developed and stable polymer system that does not provide space for microbial colonization. Under magnification, there were no bacterial morphological features such as cocci or bacilli, no round colony formations, and no clustered structures typical of microorganisms, confirming the absence of microbial growth (Gerardi et al., 2024).

Formulation A3, with the highest carrageenan concentration, exhibits the most compact and glossy surface, characterized by a uniform fine-granular texture. The distribution of bright and dark spots in the image reflects light scattering from the polymer matrix, which is strongly interconnected through a dominant coil–helix mechanism at higher carrageenan concentrations. The magnified view shows a highly homogeneous and dense matrix with no indication of large cavities or foreign aggregates. No structures resembling microorganisms such as bacilli, cocci, or biofilms, which typically appear as small rounded shapes, clusters, or mucous-like masses under light microscopy (Gerardi et al., 2024; Sharma et al., 2023) were observed. The compact and smooth surface is theoretically consistent with enhanced antibacterial potential of the composite system, as chitosan and curcumin within a more stable matrix maintain better-protected bioactivity.

None of the three formulations exhibited morphological characteristics of microbial contamination, such as bacterial cell shapes, biofilm structures, colony granules, mucous networks, or blurry aggregated regions. The color remained consistently yellow-gold due to curcumin, without changes toward brownish or blackish tones that typically indicate microbial degradation. The absence of sharply bordered dark spots or rounded structures measuring 0.5–2 μm further supports the absence of bacterial colonies (Xie et al., 2018). Across all films, the surface morphology indicated minimal degradation, and no polymer damage patterns associated with microbial activity were detected. After five months of storage, no microbial contamination was found in any of the A1–A3 formulations.

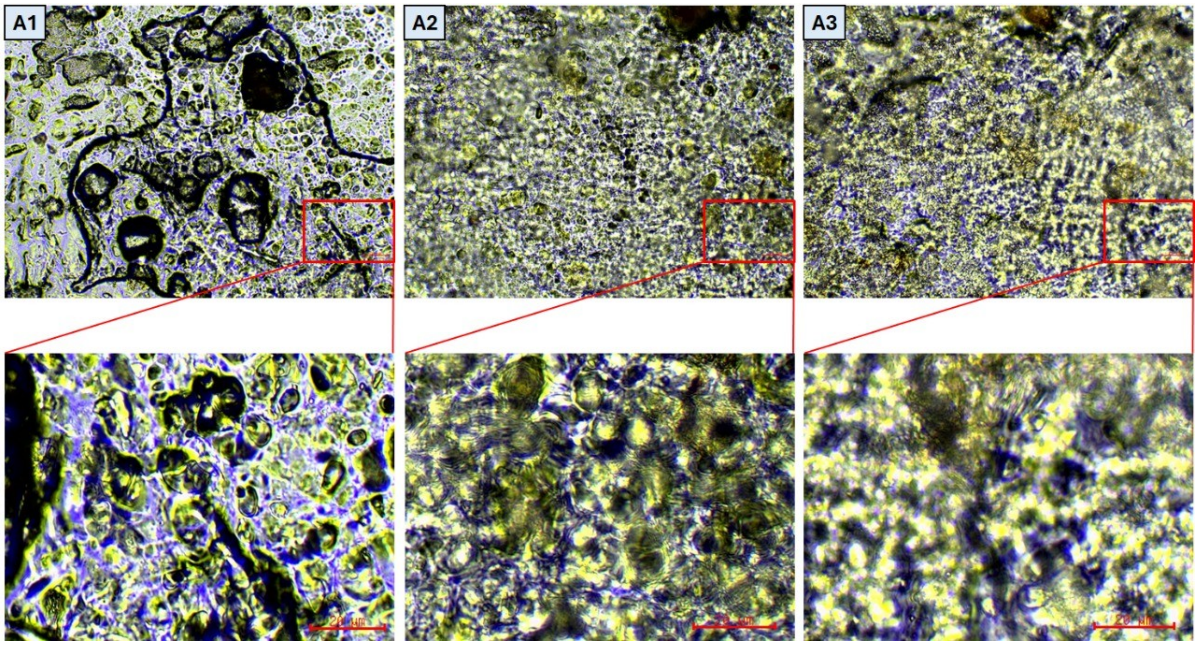

Figure 8. 3D Morphology of Hydrogel Films for Formulations A1–A3

Despite the absence of bacterial growth in all formulations, only formulation A2 maintained a morphology comparable to that depicted in Figure 7b throughout the storage period (refer to supplementary material Video S2). This observation suggests the superior structural stability of the film associated with formulation A2. Conversely, formulations A1 (refer to supplementary material video S3) and A3 (refer to supplementary material video S4) exhibited discernible alterations during storage, evidenced by the emergence of liquid on the film surface. This indicates a diminished structural stability in comparison to formulation A2.

3.4.4 Thermogravimetric Analysis

Thermal analysis using TGA and DSC was conducted to evaluate the thermal stability and phase transitions of hydrogel films A1–A3 composed of carrageenan (1–2%), chitosan (0.5%), and curcumin (0.05%). The TGA curves exhibited a stepwise weight loss pattern corresponding to moisture evaporation followed by polymer matrix degradation, where increasing carrageenan concentration from A1 to A3 resulted in enhanced thermal stability with higher residual mass. Meanwhile, DSC analysis revealed an increase in transition temperatures and thermal energy (ΔH), indicating stronger intermolecular interactions and a more compact hydrogel network at higher carrageenan content. The shifts in T_{end}, degradation peak temperature (T_{peak}), and glass transition temperature (T_g) in A3 compared to A1 confirm that increasing carrageenan concentration improves matrix compactness and thermal resistance. Overall, these findings demonstrate that polymer composition plays a critical role in determining the thermal characteristics and structural stability of hydrogel films as potential wound dressing materials, as presented in Figure 9 and Table 3.

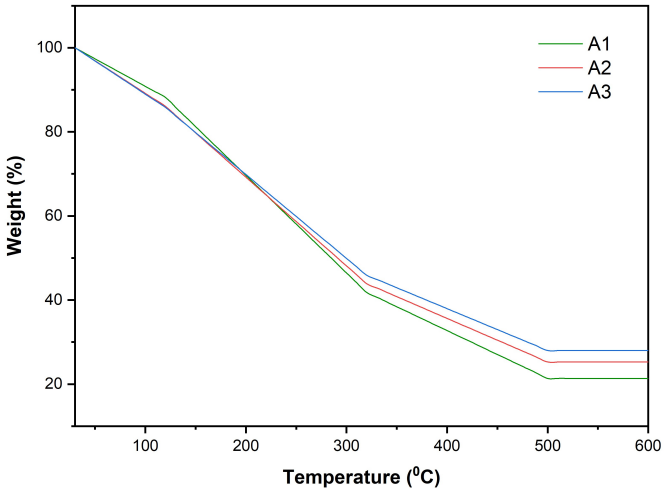

Figure 9. Thermogravimetric Analysis of Hydrogel Film Formulations (A1–A3)

Table 3. Differential Scanning Calorimetry of Hydrogel Film Formulations (A1–A3)

Parameter	A1	A2	A3
T_{end}(°C) – water loss	92.3	101.5	104.2
ΔH (J/g)	182.4	210.6	225.1
T_{peak} degradation (°C)	243.7	251.8	258.6
Tg (°C)	138.5	145.2	149.7

Thermal analysis using TGA and DSC revealed that the carrageenan/chitosan/curcumin hydrogel films exhibit a typical multi-stage degradation behavior consistent with polysaccharide-based systems (Ahmed, 2015; Hoare and Kohane, 2008). The TGA curves showed three main degradation stages, including initial water loss (30–120°C), primary polymer decomposition (200–320°C), and carbonization at higher temperatures, which are commonly observed in natural polymer-based hydrogels (Necas and Bartosikova, 2013; Rinaudo, 2006). The weight loss profile demonstrated that increasing carrageenan concentration improved thermal resistance, as reflected by lower mass loss in the main degradation stage and higher residual mass in A3 compared to A1. This trend is consistent with the formation of a denser polyelectrolyte network due to stronger ionic interactions between sulfate groups of carrageenan and protonated amine groups of chitosan, which enhances structural integrity and thermal stability (Chen et al., 2023a; Rinaudo, 2006).

The DSC results further supported this observation, where the endothermic peak associated with bound water shifted to higher temperatures (A1 < A2 < A3), indicating stronger water–polymer interactions and improved network cohesion (Ahmed, 2015). Additionally, the increase in glass transition temperature (T_g) from A1 to A3 confirms reduced chain mobility and enhanced structural rigidity due to increased crosslinking density (Hoare and Kohane, 2008). These findings are in agreement with the swelling and degradation results, where A3 exhibited the highest structural density and slowest degradation, while A1 showed the lowest stability due to its looser network structure, consistent with the correlation between crosslinking density, water retention, and degradation behavior in hydrogel systems (Chen et al., 2018; Necas and Bartosikova, 2013).

Despite the superior thermal stability observed in A3, formulation A2 demonstrates the most balanced physicochemical performance, combining sufficient thermal resistance with optimal swelling capacity and controlled degradation behavior. The moderate T_g and degradation profile of A2 indicate an ideal network density that allows efficient water retention and controlled release of bioactive compounds without excessive rigidity. This balance is crucial for wound dressing applications, where both structural stability and functional adaptability are required. Therefore, the combined TGA and DSC analyses reinforce that A2 provides the most suitable compromise between thermal stability, mechanical integrity, and biological functionality, supporting its selection as the optimal formulation for diabetic wound dressing applications.

3.5 *In Vitro* Evaluation of Hydrogel Films

3.5.1 Antibacterial Activity Assay

In vitro antibacterial activity tests were conducted on hydrogel films from formulations A0 to A3 to assess their efficacy in inhibiting the growth of *Staphylococcus aureus* and *Escherichia coli*, prevalent bacteria associated with wound infections. Notably, all three formulations demonstrated discernible inhibitory effects, with the intensity of inhibition correlating positively with the concentration of carrageenan. Specifically, formulation A2 exhibited the most pronounced inhibition zone, followed by formulation A3, A1 and formulation A0. These differences reflect the influence of the film matrix structure on the diffusion of chitosan and curcumin as active antibacterial agents, as well as the stability of bioactive compound release under testing conditions. A general overview of the antibacterial effectiveness of the three formulations is presented in Figure 10.

The *in vitro* antibacterial assay against *Staphylococcus aureus* (Gram-positive) and *Escherichia coli* (Gram-negative) demonstrated clear differences in antibacterial response among hydrogel film formulations A0, A1, A2, and A3. Based on the inhibition zone graph, formulation A2 produced the largest inhibition diameter against both bacterial strains, followed by A3, A1 and A0. The variation in antibacterial effectiveness between the two bacteria is consistent with the characteristics of their cell walls. *S. aureus* (Gram-positive) is generally more sensitive to chitosan and curcumin due to its thick peptidoglycan layer, which is permeable to cationic and phenolic molecules. In contrast, *E. coli* possesses an outer lipopolysaccharide (LPS) membrane that is more resistant to hydrophilic compounds, resulting in smaller inhibition zones compared to *S. aureus*. However, A2 still exhibited a significant increase in inhibition against both strains, indicating the success of the formulation in enhancing curcumin diffusion and improving chitosan–carrageenan interaction with microbial membranes (Rabea et al., 2003; Yallapu et al., 2012).

Chitosan in all formulations functions as the primary antibacterial agent through a direct-contact mechanism. Protonated amine groups interact with negatively charged bacterial membranes, disrupting membrane permeability and causing leakage of intracellular contents. Although the amount of chitosan is constant across formulations, its effectiveness is influenced by the carrageenan matrix, which regulates the availability of active chitosan surfaces. In formulation A2, the denser hydrogel network enhances chitosan distribution, enabling more uniform membrane contact with bacteria and resulting in stronger growth inhibition (Kong et al., 2010; Rabea et al., 2003).

The obtained data indicate that formulation A2 provides the highest and most stable antibacterial activity. Formulation A1 tends to produce a looser hydrogel network due to the low carrageenan concentration, resulting in faster and less stable curcumin release and less homogeneous chitosan distribution. Formulation A3, shows a moderate improvement in antibacterial effectiveness. In contrast, formulation A0, which consists only of carrageenan and chitosan without the addition of curcumin, shows minimal antibacterial activity. This is because, although chitosan possesses inherent antibacterial properties, its effect alone is relatively limited and less effective compared to when combined with an active compound such as curcumin. Moreover, the absence of curcumin in A0 results in no synergistic interaction that could enhance antibacterial performance. However, A2 achieves an optimal condition of polymer interaction, producing a compact film matrix, uniform component

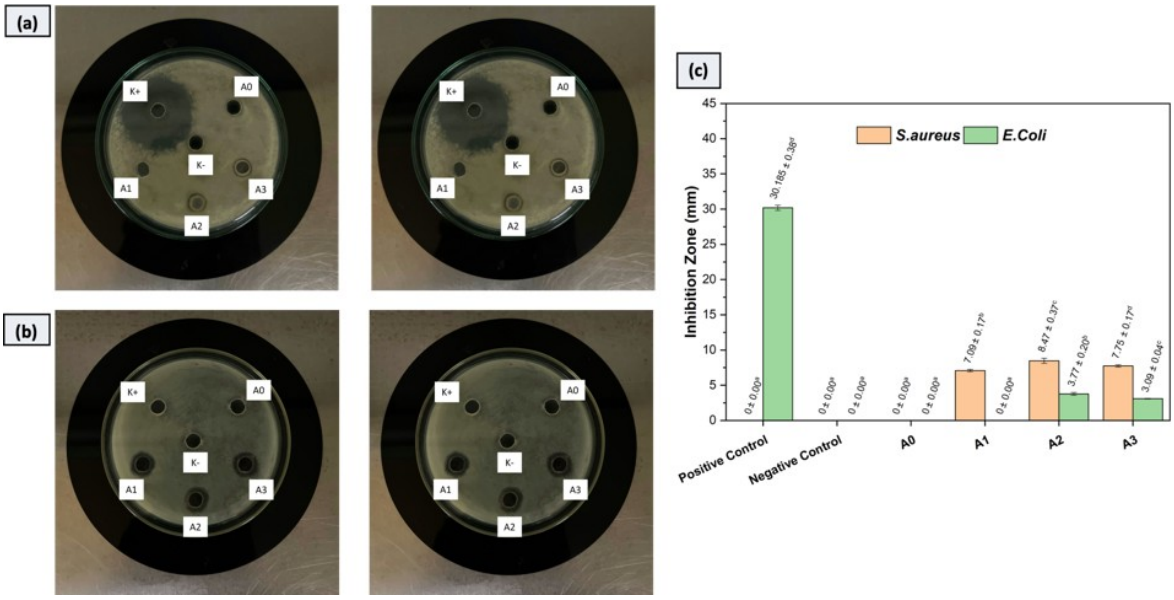

Figure 10. Qualitative Antibacterial Activity of A0–A3 Film Formulations Against *E. coli* (a) and *S. aureus* (b), Along with the Quantitative Comparison of Inhibition Zone Diameters for Both Bacteria (c)

distribution, and synergistic and more efficient release of active agents. Therefore, the antibacterial assay results not only illustrate the magnitude of the inhibition zone, but also reveal how polymer structure and component interactions determine the biological performance of the hydrogel films (Lupa et al., 2022; Xing et al., 2019).

Theoretically, the antibacterial activity of carrageenan/chitosan/curcumin hydrogel films originates from the synergistic antimicrobial mechanisms of chitosan and curcumin, facilitated by carrageenan as the structural regulator of the gel matrix. Chitosan acts as a cationic polymer capable of interacting with negatively charged bacterial membranes, disrupting membrane integrity and inducing cytoplasmic leakage. Curcumin functions as a phenolic agent with the ability to damage membranes, inhibit protein biosynthesis, and generate bactericidal free radicals. Carrageenan determines mechanical structure and release profiles of active agents through polyelectrolyte interactions with chitosan. A denser matrix, as seen in formulation A3, enhances curcumin retention and extends its diffusion period, resulting in more stable and effective antimicrobial action. This mechanism aligns with literature reporting that carrageenan/chitosan/curcumin composite hydrogels possess strong potential as bioactive wound dressings due to their combined antibacterial, anti-inflammatory, and moisture-maintaining properties (Szliszka et al., 2009; Tashakkorian et al., 2020).

MIC and MBC analyses were not conducted because the antibacterial system was developed as an intact crosslinked hydrogel film rather than a soluble antimicrobial agent. Since the antibacterial performance depends on swelling behavior and diffusion of active compounds from the polymer matrix, agar diffusion testing was considered more representative for evaluating the antimicrobial activity of the hydrogel dressing in its actual application form.

3.5.2 Antioxidant Activity Assay

In vitro antioxidant activity assays were conducted on hydrogel film formulations A0–A3 to assess the scavenging capacity of each carrageenan–chitosan–curcumin composition. This evaluation is crucial for determining the biomaterial's efficacy in mitigating oxidative stress in diabetic wounds. Variations in carrageenan concentration significantly impact the density of the hydrogel network, the release rate of curcumin, and the interaction efficiency with DPPH radicals. Consequently, these factors lead to variations in inhibition values and IC_{50} among the formulations. In general, increasing film concentration enhances the percentage of inhibition; however, formulation A2 demonstrates the most optimal performance due to a balanced matrix structure and more efficient curcumin release compared with A1 and A3. An overview of the antioxidant potential of the three hydrogel films as candidates for bioactive wound dressings can be seen in Figure 11.

The in vitro antioxidant activity assay of carrageenan /chitosan /curcumin-based hydrogel films was conducted to evaluate the ability of the three formulations (A0: 1% carrragenan and chitosan 0,5% no curcumin was added; A1: 1% carrageenan; A2: 1.5%; A3: 2%; with constant chitosan 0.5% and curcumin 0.05%) to scavenge free radicals using the DPPH method. Variations in carrageenan composition were hypothesized to influence curcumin release capacity and the formation of the polymer network, thereby directly affecting antioxidant performance. The percentage of inhibition increased with increasing film concentration for all formulations, although the increasing pattern and IC_{50} values varied. Formulation A2 exhibited the

lowest IC_{50} value (74.52 ppm), followed by A3 (133.6 ppm), A1 (162.3 ppm) and A0 (283.76), indicating that A2 possessed the strongest antioxidant activity among the three formulations, whereas A1 was the lowest. These results further affirm that the structural density of the hydrogel matrix significantly affects the release of curcumin to form an effective bond with DPPH free radicals. Thus, the carrageenan composition has fundamental implications for optimum antioxidant activity of natural-based hydrogel films to achieve high antioxidant activities.

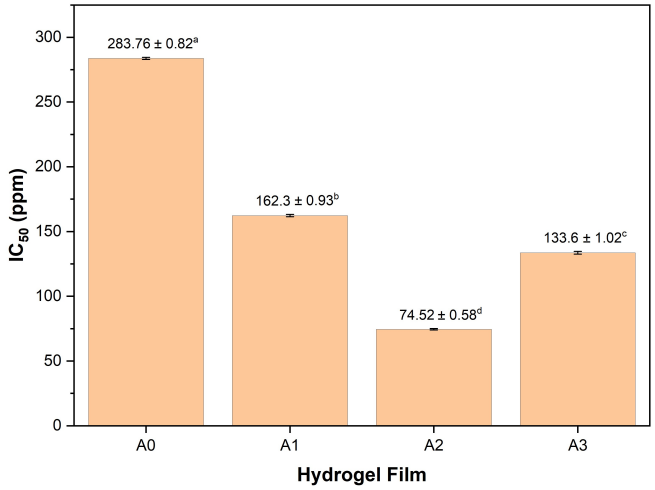

Figure 11. Antioxidant Activity of Hydrogel Film Formulations A0–A3

Inhibition patterns show differences in curcumin mobility as well as the chemical stability of the matrix and their free radicals reactivity due to different carrageenan ratios. At low carrageenan concentration (A1), curcumin will rapidly be released without sufficient amount of molecules in the reaction environment to produce any significant effect at low film concentrations. Curcumin then becomes more entrapped in the hydrogel network at relatively high carrageenan concentration (A3), necessitating significantly higher concentrations of the material for an increased antioxidant response. Formulation A0 (carrageenan–chitosan without curcumin) exhibited the highest IC_{50} value (approximately 283.76 ppm), indicating the lowest antioxidant activity among all formulations. This finding suggests that, although the base matrix components (carrageenan and chitosan) possess inherent free radical scavenging abilities, their effectiveness remains limited in the absence of an active antioxidant compound such as curcumin. Therefore, A0 can be considered a control formulation representing the intrinsic antioxidant activity of the carrageenan–chitosan matrix. However, without the incorporation of curcumin, its antioxidant performance is significantly lower. These results highlight that the presence of curcumin, along with the optimization of carrageenan ratios, plays a critical role in enhancing the antioxidant performance of the hydrogel film system. A2 reaches an optimal balance of matrix compactness and porosity, leading to the controlled and efficient release (Chen et al., 2023a; Lupa et al., 2022).

Overall, we find that the formulation A2 is the best hydrogel structure to optimize curcumin-based antioxidant performance. The lowest IC_{50} value demonstrated the best efficacy of A2 for neutralizing DPPH free radicals, and it is found in the literature that hydrogel systems including moderate polymer content impart an improved antioxidant bioavailability (Li et al., 2017; Song et al., 2022). Such a formulation is very promising as a bioactive wound dressing, according to the significance of antioxidants for the management of oxidative stress in diabetic wounds (Guo and DiPietro, 2010; Sidhu et al., 1998).

3.5.3 Percentage Release Curcumin

The analysis of curcumin release percentage from hydrogel films indicates that variations in the composition of carrageenan-chitosan-curcumin significantly influence the drug release profile within the hydrogel-based delivery system. Formulations A1 (1% carrageenan, 0.5% chitosan, 0.05% curcumin), A2 (1.5% carrageenan, 0.5% chitosan, 0.05% curcumin), and A3 (2% carrageenan, 5.5% chitosan, 0.05% curcumin) exhibit distinct release behaviors, reflecting differences in polymer network structure and density. In general, increasing carrageenan concentration tends to produce a denser hydrogel matrix, thereby slowing curcumin diffusion, whereas lower concentrations result in a faster but less controlled release. The interplay between polymer composition governs the balance between drug retention and diffusion, which is essential for achieving an effective and sustained release system in wound dressing applications. Overall, the release patterns of all formulations demonstrate a controlled and progressive mechanism, influenced by polyelectrolyte interactions and the swelling capacity of the hydrogel matrix, as described in Figure 12.

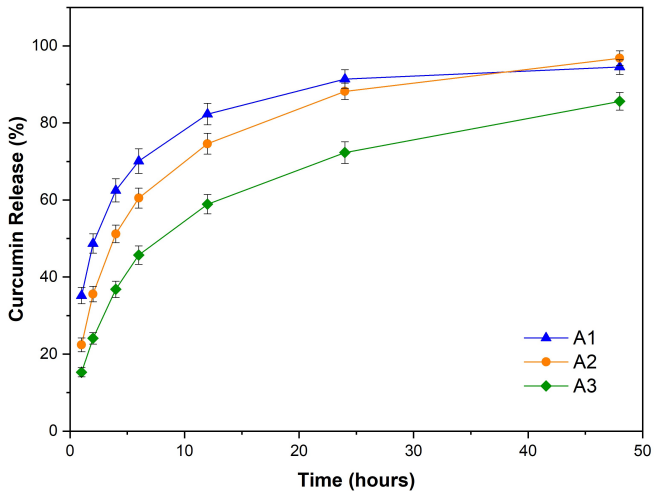

Figure 12. Percentage Release Curcumin Film Hydrogel A1-A3

Based on the analysis of the curcumin release profile and hydrogel characterization data, formulation A2 (1.5% carrageenan)

Table 4. Comparison of Hydrogel System for Wound Healing Applications

Researcher	Hydrogel System	Preparation Method	Advantages	Limitations
(Khodaei et al., 2023)	Carrageenan + oxidized polymer + dopamine + Zn^{2+}	Chemical crosslinking	Self-healing and high antibacterial activity	Lacks natural antioxidant agents
(Sharma et al., 2023)	Chitosan + CMC + nanocurcumin	Injectable hydrogel	Controlled release and accelerated wound healing	Not film-based and limited mechanical stability
(Ali et al., 2024)	Chitosan–carrageenan microbeads + curcumin	Nano-in-micro system	Effective against resistant bacteria	Complex synthesis and no film formation
(Zhang et al., 2025)	Chitosan + alginate + curcumin	Composite hydrogel	Antibacterial, antioxidant, and promotes angiogenesis	Does not include carrageenan
This study	Carrageenan + chitosan + curcumin	Casting and ionic crosslinking	Tri-component system, stable film, antibacterial and antioxidant properties, high swelling capacity, potential smart dressing	Currently limited to in vitro studies; in vivo evaluation planned

exhibits the most optimal release behavior within 24 hours, reaching approximately 88%, which reflects a balance between an adequately rapid initial release and a sustained, controlled diffusion phase. In comparison, A1 demonstrates an excessively rapid release (~92%), while A3 shows a relatively slower release (~72%). Thus, A2 provides the most stable and consistent release kinetics, supported by a homogeneous hydrogel structure, balanced porosity, and optimal polyelectrolyte interactions between carrageenan and chitosan. These findings indicate that increasing carrageenan concentration does not necessarily enhance drug release performance; instead, there exists an optimal point at which the hydrogel network density effectively regulates diffusion without excessively restricting it. Therefore, formulation A2 can be considered the most suitable candidate for diabetic wound dressing applications that require sustained curcumin release during the first 24 hours of the healing phase.

The release of curcumin from carrageenan–chitosan -based hydrogels is governed by a combination of Fickian diffusion and polymer matrix relaxation mechanisms, in which the hydrogel network structure serves as the primary regulator of the release rate. Carrageenan, as an anionic polymer, forms a gel network through double-helix associations and ionic crosslinking, while chitosan, as a cationic polymer, establishes polyelectrolyte complexes that reinforce the network structure and regulate drug molecule mobility. Within this system, curcumin is entrapped through hydrogen bonding and hydrophobic interactions, making its release dependent on the swelling degree and pore size of the hydrogel (Ahmed, 2015; Hoare and Kohane, 2008). At a moderate carrageenan concentration (A2), an optimally dense network is formed, allowing effective water penetration, polymer chain relaxation, and gradual curcumin diffusion, resulting in a stable release profile over 24 hours. In contrast, a loosely structured network (A1) leads to rapid release due to unrestricted diffusion, whereas an overly dense network (A3) restricts diffusion due to limited pore space. Therefore, modern hydrogel theory emphasizes that the balance among network density, swelling capacity, and molecular interactions is a critical determinant of the efficiency of hydrogel-based drug delivery systems, particularly for chronic wound applications such as diabetic ulcers that require controlled and sustained therapeutic release.

3.6 Comparative Studies of Hydrogel Films

Biopolymer-based hydrogels, including carrageenan, chitosan, and curcumin, have been extensively developed for wound dressing applications due to their biocompatibility and multifunctional properties. However, most studies have predominantly focused on binary systems, while investigations of ternary systems (carrageenan–chitosan–curcumin), particularly in the form of hydrogel films, remain limited and insufficiently explored. A comparative summary of previously reported hydrogel films is presented in Table 4.

In contrast, this study develops a ternary biopolymer-based hydrogel film to achieve synergistic mechanical, antibacterial, and antioxidant properties within a single system. This approach enhances structural stability and enables more controlled release of bioactive compounds, highlighting its potential as a smart wound dressing for diabetic wounds. In this regard, the novelty of this work lies in: (i) the development of a ternary natural biopolymer-based hydrogel film; (ii) the integration of mechanical, antibacterial, and antioxidant func-

tionalities within a single platform; (iii) the optimization of carrageenan composition to achieve a balanced hydrogel structure, with formulation A2 exhibiting the most favorable performance; and (iv) a comprehensive evaluation of physical, chemical, and biological properties in an integrated manner.

4. CONCLUSION

This study successfully developed carrageenan/chitosan/curcumin hydrogel films as stimulus-responsive smart materials for diabetic wound dressings, demonstrating promising physicochemical characteristics and bioactivity. Characterization confirmed κ-carrageenan in its potassium salt form with an optimal S/K ratio for gelation, heterogeneous particle distribution influencing hydration kinetics, and distinctive spectroscopic markers supporting the formation of a stable three-dimensional network. Among the three formulations, A2 with 1.5% carrageenan exhibited the most optimal balance, with a thickness of 0.20 mm, moisture content of approximately 20%, physiological pH, controlled swelling kinetics reaching 1439%, and slow degradation indicating superior mechanical stability. The compact and homogeneous microstructure of A2 supports the controlled release of bioactive agents. Film A2 demonstrated the highest antibacterial activity against *Staphylococcus aureus* (8.47 mm inhibition zone) and *Escherichia coli* (3.77 mm), as well as the strongest antioxidant activity with an IC_{50} value of 74.52 ppm. The synergy between carrageenan as a hydrophilic matrix, chitosan as an antimicrobial agent, and curcumin as an antioxidant results in a multifunctional system that integrates antimicrobial protection, oxidative stress mitigation, and exudate management to address the complex pathophysiology of diabetic wounds.

5. ACKNOWLEDGMENT

The authors gratefully acknowledge the Directorate of Research and Community Service, Ministry of Higher Education, Science, and Technology, for its financial support through the 2025 Fundamental Research Scheme, awarded under Decree No. 0419/C3/DT.05.00/2025 and Contract No. 129/C3/DT .05.00/PL/2025; 2166/LL8/AL.04/2025; and 011/LPPM Unswa/VI/2025.

REFERENCES

Ahmed, E. M. (2015). Hydrogel: Preparation, Characterization, and Applications: A Review. *Journal of Advanced Research*, **6**(2); 105–121

Ali, S. M. A., J. Khan, R. Shahid, S. Shabbir, M. F. Ayoob, and M. Imran (2024). Chitosan-Carrageenan Microbeads Containing Nano-Encapsulated Curcumin: Nano-in-Micro Hydrogels as Alternative-Therapeutics for Resistant Pathogens Associated With Chronic Wounds. *International Journal of Biological Macromolecules*, **278**; 134841

Amine, C., A. Boire, A. Kermarrec, and D. Renard (2019). Associative Properties of Rapeseed Napin and Pectin: Competition Between Liquid-Liquid and Liquid-Solid Phase Separation. *Food Hydrocolloids*, **92**; 94–103

Aranaz, I., A. R. Alcántara, M. C. Civera, C. Arias, B. Elorza, A. Heras Caballero, and N. Acosta (2021). Chitosan: An Overview of Its Properties and Applications. *Polymers*, **13**(19); 3256

Atgié, M., J. C. Garrigues, A. Chennevière, O. Masbernat, and K. Roger (2019). Gum Arabic in Solution: Composition and Multi-Scale Structures. *Food Hydrocolloids*, **91**; 319–330

Boateng, J. S., K. H. Matthews, H. N. E. Stevens, and G. M. Eccleston (2008). Wound Healing Dressings and Drug Delivery Systems: A Review. *Journal of Pharmaceutical Sciences*, **97**(8); 2892–2923

Brett, D. W. (2006). A Review of Moisture-Control Dressings in Wound Care. *Journal of Wound, Ostomy & Continence Nursing*, **33**(Supplement 6S); S3–S8

Campo, V. L., D. F. Kawano, D. B. D. Silva, and I. Carvalho (2009). Carrageenans: Biological Properties, Chemical Modifications and Structural Analysis – A Review. *Carbohydrate Polymers*, **77**(2); 167–180

Chen, A., S. Deng, J. Lai, J. Li, W. Chen, S. N. Varma, J. Zhang, C. Lei, C. Liu, and L. Huang (2023a). Hydrogels for Oral Tissue Engineering: Challenges and Opportunities. *Molecules*, **28**(9); 3946

Chen, H., J. Cheng, L. Ran, K. Yu, B. Lu, G. Lan, F. Dai, and F. Lu (2018). An Injectable Self-Healing Hydrogel With Adhesive and Antibacterial Properties Effectively Promotes Wound Healing. *Carbohydrate Polymers*, **201**; 522–531

Chen, Y., X. Wang, S. Tao, Q. Wang, P.-Q. Ma, Z.-B. Li, Y.-L. Wu, and D.-W. Li (2023b). Research Advances in Smart Responsive-Hydrogel Dressings With Potential Clinical Diabetic Wound Healing Properties. *Military Medical Research*, **10**(1); 37

Escárcega-Galaz, A. A., D. I. Sánchez-Machado, J. López-Cervantes, A. Sanches-Silva, T. J. Madera-Santana, and P. Paseiro-Losada (2018). Mechanical, Structural and Physical Aspects of Chitosan-Based Films as Antimicrobial Dressings. *International Journal of Biological Macromolecules*, **116**; 472–481

Gao, D., Y. Zhang, D. T. Bowers, W. Liu, and M. Ma (2021). Functional Hydrogels for Diabetic Wound Management. *APL Bioengineering*, **5**(3); 031503

Gerardi, D., S. Bernardi, A. Bruni, G. Falisi, and G. Botticelli (2024). Characterization and Morphological Methods for Oral Biofilm Visualization: Where Are We Nowadays? *AIMS Microbiology*, **10**(2); 391–414

Guo, S. and L. A. DiPietro (2010). Factors Affecting Wound Healing. *Journal of Dental Research*, **89**(3); 219–229

Han, C., R. K. Singla, and C. Wang (2025). Application of Biomaterials in Diabetic Wound Healing: The Recent Advances and Pathological Aspects. *Pharmaceutics*, **17**(10); 1295

He, X., Y. Wei, and K. Xu (2025). Hydrogel-Based Treatment of Diabetic Wounds: From Smart Responsive to Smart Monitoring. *Gels*, **11**(8); 647

Hidayaty, A. N., S. Fiddaroini, A. L. Fahmi, Q. Fardiyah, and

A. Sabarudin (2026). Optimization and Stability Assessment of Chitosan/PVA Smart Sensor Films Incorporated With Roselle Anthocyanins for Real-Time Visual Monitoring of Chicken and Shrimp Freshness Under Different Storage Conditions. *Science and Technology Indonesia*, **11**(1); 217–234

Hoare, T. R. and D. S. Kohane (2008). Hydrogels in Drug Delivery: Progress and Challenges. *Polymer*, **49**(8); 1993–2007

Hossain, M. J., M. Al-Mamun, and M. R. Islam (2024). Diabetes Mellitus, the Fastest Growing Global Public Health Concern: Early Detection Should Be Focused. *Health Science Reports*, **7**(3); e2004

Jin, X., W. Lan, W. Yong, Z. Yuan, X. Li, and X. Cui (2026). Application and Development of Stimulus-Responsive Hydrogel Biomaterials for Diabetic Wound Healing: A Literature Review. *Frontiers in Medicine*, **12**; 1740559

Khodaei, T., J. Nourmohammadi, A. Ghaee, and Z. Khodaii (2023). An Antibacterial and Self-Healing Hydrogel From Aldehyde-Carrageenan for Wound Healing Applications. *Carbohydrate Polymers*, **302**; 120371

Kong, M., X. G. Chen, K. Xing, and H. J. Park (2010). Antimicrobial Properties of Chitosan and Mode of Action: A State of the Art Review. *International Journal of Food Microbiology*, **144**(1); 51–63

Li, G., Q. Xiao, L. Zhang, Y. Zhao, and Y. Yang (2017). Nerve Growth Factor Loaded Heparin/Chitosan Scaffolds for Accelerating Peripheral Nerve Regeneration. *Carbohydrate Polymers*, **171**; 39–49

Liu, Z., Y. Lv, G. Zheng, W. Wu, and X. Che (2023). Chitosan/Polylactic Acid Nanofibers Containing Astragaloside IV as a New Biodegradable Wound Dressing for Wound Healing. *AAPS PharmSciTech*, **24**(7); 202

Lupa, D., W. Płaziński, A. Michna, M. Wasilewska, P. Pomastowski, A. Gołębiowski, B. Buszewski, and Z. Adamczyk (2022). Chitosan Characteristics in Electrolyte Solutions: Combined Molecular Dynamics Modeling and Slender Body Hydrodynamics. *Carbohydrate Polymers*, **292**; 119676

Madaniyah, L., S. Fiddaroini, E. K. Hayati, M. F. Rahman, and A. Sabarudin (2025). Stability of Biologically Synthesized Silver Nanoparticles (AgNPs) Using *Acalypha indica* L. Plant Extract as Bioreductor and Their Potential as Anticancer Agents Against T47D Cells. *Science and Technology Indonesia*, **10**(1); 101–110

Necas, J. and L. Bartosikova (2013). Carrageenan: A Review. *Veterinární Medicína*, **58**(4); 187–205

Nešporová, K., V. Pavlík, B. Šafránková, H. Vágnerová, P. Odráška, O. Žídek, N. Císařová, S. Skoroplyas, L. Kubala, and V. Velebný (2020). Effects of Wound Dressings Containing Silver on Skin and Immune Cells. *Scientific Reports*, **10**(1); 15216

Priyadarsini, K. (2014). The Chemistry of Curcumin: From Extraction to Therapeutic Agent. *Molecules*, **19**(12); 20091–20112

Rabea, E. I., M. E.-T. Badawy, C. V. Stevens, G. Smagghe, and W. Steurbaut (2003). Chitosan as Antimicrobial Agent: Applications and Mode of Action. *Biomacromolecules*, **4**(6); 1457–1465

Reig-Vano, B., B. Tylkowski, X. Montané, and M. Giamberini (2021). Alginate-Based Hydrogels for Cancer Therapy and Research. *International Journal of Biological Macromolecules*, **170**; 424–436

Rinaudo, M. (2006). Chitin and Chitosan: Properties and Applications. *Progress in Polymer Science*, **31**(7); 603–632

Rizky, A., D. Tanjung, and K. Khairunnisa (2024). The Effect of Ozone Therapy Stimulation on Diabetes Wound Healing Process. *Contagion: Scientific Periodical Journal of Public Health and Coastal Health*, **6**(1); 480

Rupert, R., K. F. Rodrigues, V. Y. Thien, and W. T. L. Yong (2022). Carrageenan From Kappaphycus alvarezii (Rhodophyta, Solieriaceae): Metabolism, Structure, Production, and Application. *Frontiers in Plant Science*, **13**; 859635

Shah, S. A., M. Sohail, M. Karperien, C. Johnbosco, A. Mahmood, and M. Kousar (2023). Chitosan and Carboxymethyl Cellulose-Based 3D Multifunctional Bioactive Hydrogels Loaded With Nano-Curcumin for Synergistic Diabetic Wound Repair. *International Journal of Biological Macromolecules*, **227**; 1203–1220

Sharma, S., J. Mohler, S. D. Mahajan, S. A. Schwartz, L. Bruggemann, and R. Aalinkeel (2023). Microbial Biofilm: A Review on Formation, Infection, Antibiotic Resistance, Control Measures, and Innovative Treatment. *Microorganisms*, **11**(6); 1614

Sidhu, G. S., A. K. Singh, D. Thaloor, K. K. Banaudha, G. K. Patnaik, R. C. Srimal, and R. K. Maheshwari (1998). Enhancement of Wound Healing by Curcumin in Animals. *Wound Repair and Regeneration*, **6**(2); 167–177

Song, Y., J. Y. Seo, H. Kim, S. Cho, and K.-Y. Baek (2022). Pore-Size Control of Chitin Nanofibrous Composite Membrane Using Metal-Organic Frameworks. *Carbohydrate Polymers*, **275**; 118754

Sweeney, I. R., M. Miraftab, and G. Collyer (2012). A Critical Review of Modern and Emerging Absorbent Dressings Used to Treat Exuding Wounds. *International Wound Journal*, **9**(6); 601–612

Szliszka, E., Z. P. Czuba, M. Domino, B. Mazur, G. Zydowicz, and W. Krol (2009). Ethanolic Extract of Propolis (EEP) Enhances the Apoptosis-Inducing Potential of TRAIL in Cancer Cells. *Molecules*, **14**(2); 738–754

Tashakkorian, H., V. Hasantabar, A. Mostafazadeh, and M. Golpour (2020). Transparent Chitosan Based Nanobiocomposite Hydrogel: Synthesis, Thermophysical Characterization, Cell Adhesion and Viability Assay. *International Journal of Biological Macromolecules*, **144**; 715–724

Tian, W., L. Dai, S. Lu, Z. Luo, Z. Qiu, J. Li, P. Li, and B. Du (2019). Effect of Bacillus sp. DU-106 Fermentation on Dendrobium officinale Polysaccharide: Structure and Immunoregulatory Activities. *International Journal of Biological Macromolecules*, **135**; 1034–1042

Vilchez, A., F. Acevedo, M. Cea, M. Seeger, and R. Navia

(2021). Development and Thermochemical Characterization of an Antioxidant Material Based on Polyhydroxybutyrate Electrospun Microfibers. *International Journal of Biological Macromolecules*, **183**; 772–780

Xie, W., X. Meng, Y. Zhai, P. Zhou, T. Ye, Z. Wang, G. Sun, and X. Sun (2018). Panax Notoginseng Saponins: A Review of Its Mechanisms of Antidepressant or Anxiolytic Effects and Network Analysis on Phytochemistry and Pharmacology. *Molecules*, **23**(4); 940

Xing, J., P. Tao, Z. Wu, C. Xing, X. Liao, and S. Nie (2019). Nanocellulose-Graphene Composites: A Promising Nanomaterial for Flexible Supercapacitors. *Carbohydrate Polymers*, **207**; 447–459

Yallapu, M. M., M. Jaggi, and S. C. Chauhan (2012). Curcumin Nanoformulations: A Future Nanomedicine for Cancer. *Drug Discovery Today*, **17**(1–2); 71–80

Zhang, X., Y. Liu, Z. Wang, H. Zhao, L. Zhan, H. Gui, X. Xu, X. Ma, and B. Ma (2025). pH-Responsive and Self-Adaptive Injectable Sodium Alginate/Carboxymethyl Chitosan Hydrogel Accelerates Infected Wound Healing by Bacteriostasis and Immunomodulation. *Carbohydrate Polymers*, **354**; 123322

